frontiers | Frontiers in Earth Science

TYPE Original Research
PUBLISHED 01 February 2023
DOI 10.3389/feart.2022.1008707

OPEN ACCESS

EDITED BY
Xing Xu,
Yunnan University, China

REVIEWED BY
Li Tian,
China University of Geosciences Wuhan, China
Daoliang Chu,
China University of Geosciences Wuhan, China

*CORRESPONDENCE
Yuewu Sun,
sunyuewu@jlu.edu.cn

SPECIALTY SECTION
This article was submitted to Paleontology, a section of the journal Frontiers in Earth Science

RECEIVED 01 August 2022
ACCEPTED 21 November 2022
PUBLISHED 01 February 2023

CITATION
Li X, Zhang Y, Sun Y, Shi X and Zhang S (2023), Vegetation changes and climate shift during the latest Ladinian to the early Carnian: Palynological evidence from the Yanchang Formation, Ordos Basin, China. *Front. Earth Sci.* 10:1008707.
doi: 10.3389/feart.2022.1008707

Vegetation changes and climate shift during the latest Ladinian to the early Carnian: Palynological evidence from the Yanchang Formation, Ordos Basin, China

Xiang Li[1], Ying Zhang[2], Yuewu Sun[2,3,4]*, Xiao Shi[1] and Shuqin Zhang[3]

[1]College of Earth Sciences, Jilin University, Changchun, China, [2]International Centre for Geoscience Research and Education in Northeast Asia, Jilin University, Changchun, China, [3]Research Center of Palaeontology and Stratigraphy, Jilin University, Changchun, China, [4]Key-Lab for Oil Shale and Paragenetic Minerals of Jilin Province, Changchun, China

The Middle–Late Triassic climates have attracted the attention of paleontological and geological scientists for the Carnian pluvial event in the early Late Triassic. The event is well-documented in the pelagic and epi-continental marine deposits of the Tethys, Gondwana, and Laurasia. However, inland terrestrial deposits are less frequently depicted, with high-resolution palynological biostratigraphy constraints. In this study, we report the palynological records from the YC8-1 and YC7-3 sub-members of the Yunmeng profile in the Ordos Basin, China, where the YC7-3 was dated at 236.0–234.1 Ma. Two palynological assemblages were recognized and named the *Lundbladispora watangensis–Taeniaesporites combinatus* assemblage and *Lundbladispora communis–Discisporites granulus* assemblage for the YC8-1 and YC7-3 sub-members, respectively. Their ages were determined to be the latest Ladinian and early Carnian, respectively, for their stratigraphic correlations with the global boundary stratotype section and point (GSSP) of the base of Carnian in Europe and additional co-occurring floras with condonts in the Upper Triassic of South China. The coexistence of *Cyathidites minor* (Couper, 1953), *Dictyophyllidites harrisii* (Couper, 1958), *Apiculatisporis bulliensis* (Helby ex De Jersey, 1972), *Aratrisporites xiangxiensis* (Li and Shang, 2011), *Piceaepollenites omoriciformis* (Bolkh.) (Xu and Zhang, 1984), *Podocarpidites ornatus* (Pocock, 1962), *Discisporites granulus* (Zhang, 1984), and *Classopollis* (Pflug, 1953) is equivalent to the Carnian palynostratigraphic criterion reported in the North China palynofloristic realm. Vegetational changes, especially those occurring at the boundary between Ladinian and Carnian, account for approximately 70% of ferns and over 30% of gymnosperms lost. These were discovered and attributed to the strong seasonal arid climate, indicated by the emergence of Cheirolepidiaceae and *Pinuspollenites*. We thus know that the climate during the latest Ladinian and early Carnian was "hot house" with seasonal aridity. In addition, three strong monsoonal pluvial pulses were signaled by the humidity index of lowland plants. The present study will enable a better understanding the Carnian pluvial event in the Late Triassic inland basin.

KEYWORDS

Carnian pluvial event, arid climate, megamonsoon, Triassic, Ordos inland basin, palynology, Ladinian–Carnian boundary, Yanchang Formation

1 Introduction

While the Triassic period (201.3–252 Ma; Benton and Newell, 2014) might be "hot house" period, as evidenced by ice-free poles covered by green forests (Harris, 1937; Vasilevskaya, 1972; Smith, 1974; Harland, 1997; Cuneo et al., 2003; Strullu-Derrien et al., 2012), eolian deserts were widespread in tropical and subtropical areas during the Early and Middle Triassic, with green vegetation present only along permanent rivers (termed "gallery forest"; Zhu et al., 2020; Shi et al., 2021). The most important plate tectonic event occurred in the tropical Tethys realm, represented by the closure of the Paleo-Tethys and opening of the Neo-Tethys during the Triassic period (Boucot et al., 2009; Domeier and Torsvic, 2014). The climate of the supercontinent Pangea was characterized by a mega-monsoonal circulation which reached its maximum volume in the Triassic (Kutzbach and Gallimore, 1989; Parrish, 1993).

Meanwhile, in the circum-Paleo-Tethys area during the Early and Middle Triassic, the climate might have been like the Mediterranean of today. Hot and dry summers might have eliminated most plant life from the winter ponds, which were inhabited by small hydrophytic quillworts and surrounded by lycopod shrubs and small conifers (Retallack, 1997). Thence, the Late Triassic climate changed to pluvial, with green vegetation and coal deposits overlying the former red continental sediments (Boucot et al., 2009). Frequent floods may have led to the formation of black organic-rich shale in lakes and the Panthalassa seacoast (Hornung and Brandner, 2005; Liu et al., 2022)—a notable characteristic of the Carnian Pluvial Event (CPE) (Simms and Ruffell, 1990). The palynoflora, both in the tropical Tethys (Dubiel et al., 1991; Shi et al., 2009; Preto et al., 2010; Wang et al., 2012; Mueller et al., 2016) and boreal areas (Mueller et al., 2015), and even in the middle latitudes of Gondwana (Césari and Colombi, 2016; Colombi et al., 2021), recorded vegetation and climate changes in the seasonal paleoclimate's rainfall during the CPE. As it coincided with negative carbon isotopic excursion (Dal Corso et al., 2012; Dal Corso et al., 2015), the CPE has been attributed to the release of CO_2 from large volcanic eruptions (Dal Corso et al., 2012; Dal Corso et al., 2015; Mueller et al., 2016).

This study presents the results of a palynological investigation of lacustrine deposits that were calibrated as early Carnian by U-Pb isotopic dating of bentonites in the Ordos Basin, China (Figure 1), in order to shed new light on our understanding of the CPE in the Late Triassic inland basin.

2 Geological setting

Located in the eastern realm of the Paleo-Tethys, the Triassic Ordos Basin was situated at 18.3–25.4°N (Ma et al., 1993) in the North China Craton. The basin was derived from an epi-continental sea that developed during the Late Carboniferous to Middle Triassic. The Ordos became a foreland basin due to the collision of the South and the North China Cratons along the Mianlue suture from approximately 250 Ma; however, recent detrital zircon U-Pb isotope dating of the early Late Triassic Yanchang Formation shows that the protoliths were sourced only from the North China Craton and not the South China Craton and the Qinling Orogenic Belt (Xie and Heller, 2013). The deposition of Triassic sediments in the Ordos Basin can be divided into two cycles (IGCAGS, 1980; PCOC, 1992): 1) the Lower and Middle Triassic cycles, including the Liujiagou, Heshanggou, and Ermaying formations, which are widespread throughout the entire North China Craton; 2) the Upper Triassic cycle composed of the Yanchang Formation (*sensu lato*) comprising alluvial, fluvial, deltaic, and lacustrine sedimentary rocks, approximately 1,000–1,300 m in thickness. The Yanchang Formation (Pan, 1934) or Group (ECSDC, 2000) can be divided into five members (Y1–Y5) (IGCAGS, 1980) and 10 oil layers or members (YC1–YC10), based on the depositional sequences (S1–S5), regional and local indicator beds (K0–K9), and bentonite beds (B0–B6) (PCOC, 1992; Pang et al., 2010; Yang et al., 2017; Deng et al., 2018; Zhang et al., 2019; Sun et al., 2020). The Chang 7 oil layer (member) of the Yanchang Formation (YC7) is one of the best layers of source rocks in the Ordos Basin (PCOC, 1992), shale oil being the most important fossil energy source in China and elsewhere (Jin et al., 2019; Liu et al., 2022). YC7 shale oil is deposited in deep or semi-deep lacustrine environments when the basin extends to its maximum; known as "Zhangjiatan Shale," it is also a regional marker for stratigraphic correlation. The shale has also been proposed for the division of Triassic strata and their geological age. Its presence was assigned to the uppermost Tongchuan Formation (IGCAGS, 1980; Tong et al., 2019) or the lowest Yongping Formation (Li et al., 2016), while its age was assigned to either the Middle (IGCAGS, 1980; Deng et al., 2018) or Late Triassic (Li et al., 2016; Tong et al., 2019; Sun et al., 2020). However, the Yanchang Formation (*sensu lato*) is widely used (Bureau of Geology and Mineral Resources of Shaanxi Province, 1998) in geological references (Table 1). The formation conformably overlies the Middle Triassic Ermaying Formation (or Zhifang Formation), which is characterized by purple or grayish-red siltstones and mudstones intercalated within grayish and yellowish-green sandstones.

3 Materials and methods

Palynological samples were collected from the Yunmeng profile (GPS: N 35°15′58.87″, E 109°13′50.7″, H 1,298.45 m) which was manually outcropped at Ruzhihe Village in Yunmeng Town, Yijun County, Tongchuan City, Shaanxi Province, northwestern China (Figure 1). YC8 and YC7 on the profile are construed as Middle and Late Triassic in age, respectively (Ji and Meng, 2006; Sun et al., 2020). The total thickness of the measured Yunmeng profile is >30 m (Supplementary Figure S1). Some 27 palynological samples were collected from the black shale layers of YC8-1 (9.01 m thick and dominated by gray fine-grained sandstone and siltstone), and 60 samples were collected from YC7-3 (21.29 m thick and mainly composed of dark gray, brown oil-shale, shale, and thin-layered bentonite).

Each 50 g sample was broken into pieces <1.0 mm in diameter and treated with HCl (30%) for 24 h and HF (36%) for 2 days. ZnCl-mixed KI heavy liquid (2.2 g/cm^3) and an 8 μm sieve were used to separate the organic residue from minerals and gather the palynomorphs. All samples, slides, and stubs numbered with the prefix STYM were housed in the Research Center of Paleontology and Stratigraphy, Jilin University, China. Details of the samples are provided in Supplementary Appendix S1.

4 Results

4.1 Palynological assemblages

Among the 87 palynological samples collected from the Yunmeng profile, only 15 samples containing over 100 grains of

10.3389/feart.2022.1008707

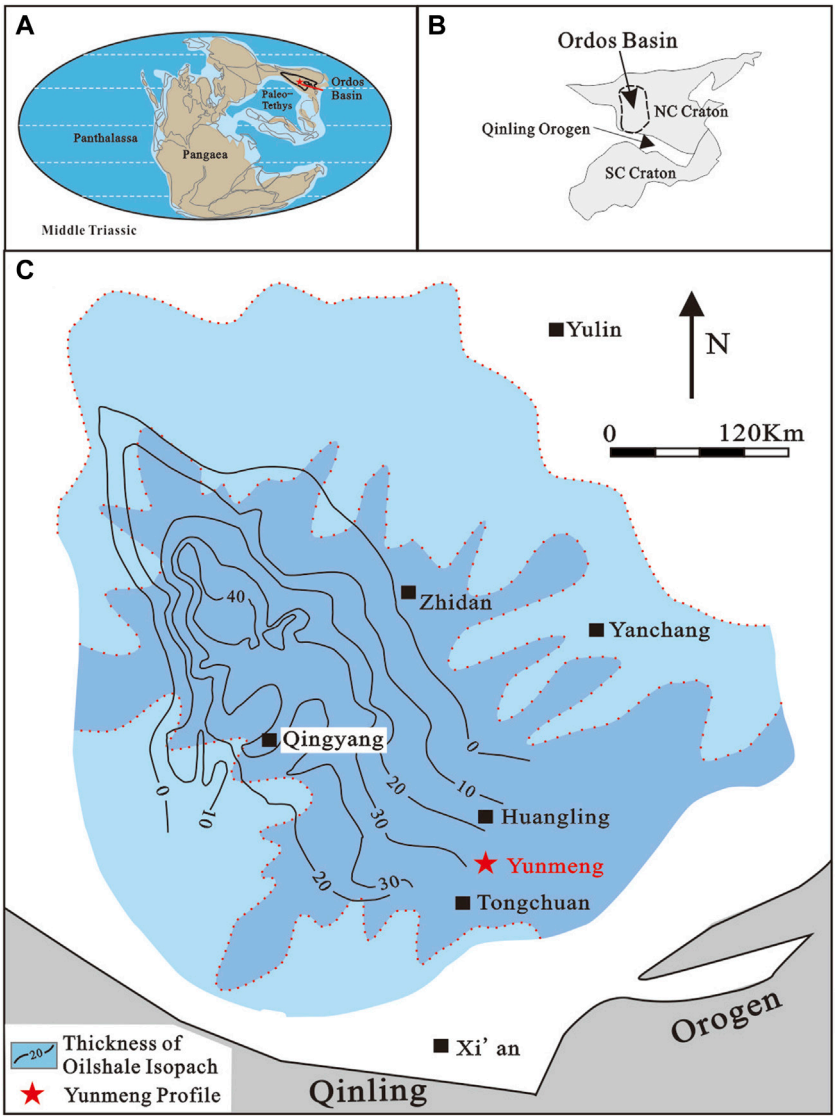

FIGURE 1
Geographical and geological location of the Yunmeng Profile in the Ordos Basin (after Sun et al., 2020). **(A)** Reconstructed topography in late Middle Triassic (after Zhang et al., 2019). **(B)** Geographic map of China showing location of the Ordos Basin; NC Craton, North China Craton; SC Craton, South China Craton. **(C)** Paleogeographic map of YC7 showing the isopach of oil-shale.

pollen and spores were quantitatively analyzed. A total of 45 species assigned to 24 genera (Figures 2–4) were described; their botanical affinity is shown in Supplementary Appendix S2. Their relative abundance was calculated using TiLIA software (2.1.1). Two palynological assemblages were recognized using CONISS within TiLIA (Grimm, 1991–2016) in ascending order (Figure 5).

4.1.1 *Lundbladispora watangensis–Taeniaesporites combinatus* assemblage (WC)

This palynological assemblage comprised 10 samples collected from the YC8-1 sub-member in the Yunmeng profile, from which 1,092 specimens were identified. The taxa in this assemblage comprised 121 species of 47 genera, including spores of 54 species belonging to 17 genera and pollens of 67 species belonging to 30 genera, respectively (Supplementary Appendix S1).

The fern spores (21%–48%) in the WC palynological assemblage mainly belonged to *Lundbladispora* (5%–20%), *Aratrisporites* (2%–10%), *Verrucosisporites* (0%–11%), *Cyclogranisporites* (1%–8%), *Duplexisporites* (0%–6%), and *Calamospora* (0%–6%). The dominant species were *L. watangensis* (0%–6%), *L. playfordi* (0%–5%), *Aratrisporites tenuispinosus* (0%–6%), *A. granulates* (0%–3%), *Verrucosisporites krempii* (0%–6%), *V. scitulus* (0%–5%), *Duplexisporites rotundatus* (0%–6%), *Kraeuselisporites apiculatus* (0%–5%), and *Asseretospora gyrata* (0%–2%). The pollen (52%–79%) in the WC assemblage mainly comprised *Taeniaesporites* (2%–18%), *Chasmatosporites* (4%–16%), and *Alisporites* (3%–13%), as well as *Platysaccus* (1%–5%), *Striatoabieites* (0%–7%), *Podocarpidites* (0%–7%), *Ovalipollis* (0%–7%), *Klausipollenites* (0%–6%), *Piceaepollenites* (0%–4%), *Cycadopites* (0%–3%), and *Cedripites* (0%–3%). The most important species of pollen in the WC assemblage

TABLE 1 Historical division of the Yanchang Formation (*sensu lato*) in Ordos Basin, China.

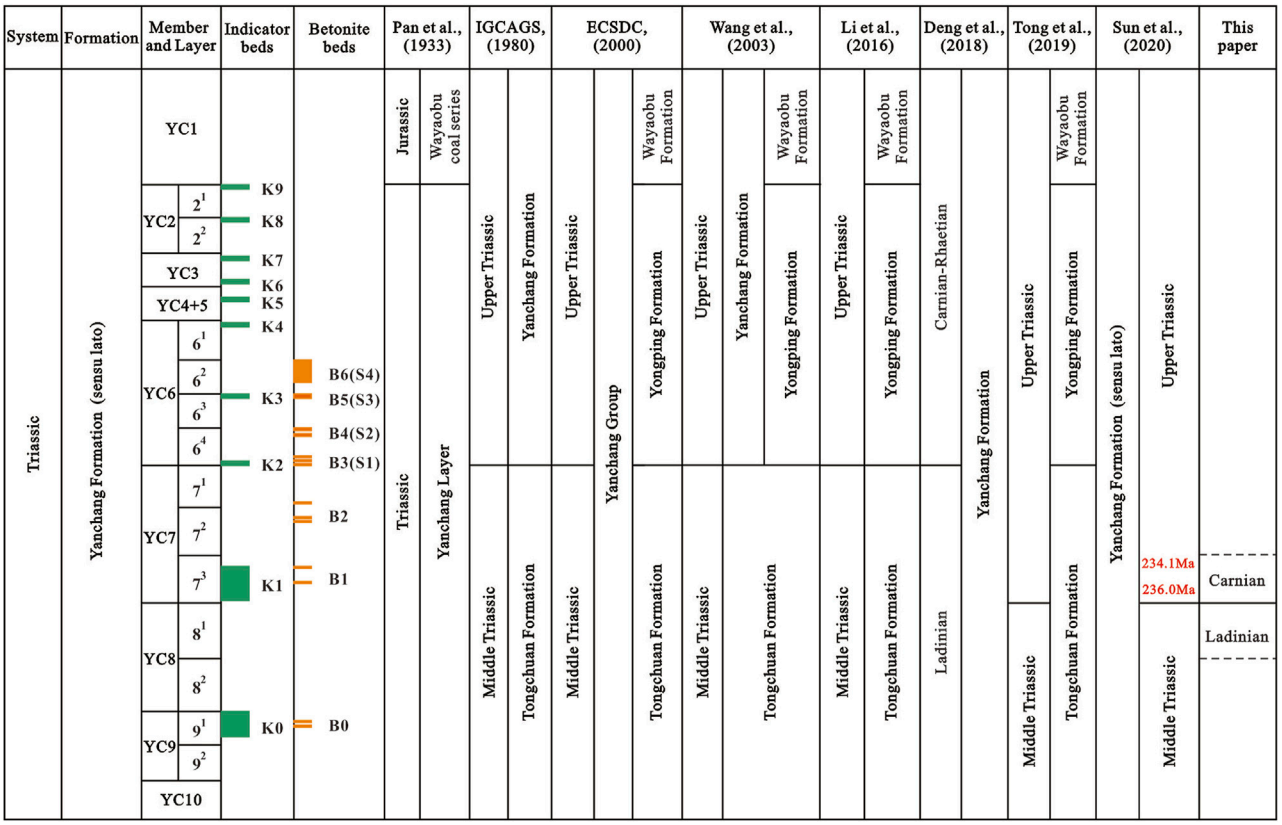

were *Taeniaesporites combinatus* (0%–9%), *T. watangensis* (0%–1%), *Alisporites aequalis* (0%–5%), *Platysaccus proximus* (0%–3%), *P. queenslundi* (0%–2%), *Striatoabieites duivenii* (0%–2%), *Ovalipollis ovalis* (0%–4%), *O. breviformis* (0%–3%), *Podocarpidites paulus* (0%–2%), and *Cycadopites typicus* (0%–2%).

4.1.2 *Lundbladispora communis–Discisporites granulus* assemblage (CG)

This palynological assemblage comprised 20 samples collected from the YC7-3 sub-member in the Yunmeng profile, from which 1,083 specimens were identified. The taxa in this assemblage were less diversified, with only 76 species of 45 genera in total, including spores of 22 species belonging to 13 genera and pollen of 54 species belonging to 32 genera (Supplementary Appendix S1).

Fern spores (20%–39%) in the CG palynological assemblage mainly consisted of *Lundbladispora* (4%–12%), *Cyclogranisporites* (2%–8%), *Dictyophyllidites* (0%–5%), *Aratrisporites* (1%–3%), *Kraeuselisporites* (0%–3%), *Lunzisporites* (0%–5%), and *Cyathidites* (0%–1%). Common species identified were *Lundbladispora communis* (0%–4%), *L. playfordi* (1%–4%), *Dictyophyllidites harrisii* (0%–5%), *Duplexisporites rotundatus* (0%–6%), *Lunzisporites sparsus* (0%–5%), and *Kraeuselisporites spinosus* (0%–3%). Pollen (52%–79%) in the CG assemblage mainly comprised *Ovalipollis* (3%–13%), *Discisporites* (0%–17%), *Protopinus* (5%–11%), and *Pristinuspollenites* (0%–12%). *Alisporites* (2%–8%), *Klausipollenites* (1%–8%), *Podocarpidites* (0%–7%), *Platysaccus* (2%–5%), and *Cycadopites* (3%–7%) were common. The most important pollens (with stratigraphic significance) in the CG assemblage were *Discisporites granulus* (0%–4%), *Cycadopites typicus* (1%–3%), *Ovalipollis ovalis* (1%–3%), *Klausipollenites schaubergeri* (0%–3%), and *P. queenslundi* (0%–2%).

4.2 Comparison of the palynological assemblages in the Ordos Basin

Qu (1980) and Liu et al. (1981) reported palynological assemblages from the upper member of the Tongchuan Formation on the Qishuihe profile near the Yunmeng profile. These were characterized by abundant fern spores (66.8%–77%) represented by *Verrucosisporites* (8.3%–16.7%), *Punctatisporites* (33.2%), and *Todisporites* (46.5%) (Qu, 1980; Liu et al., 1981). *Aratrisporites* are normally rare in the Qishuihe profile, whereas they are abundant (13%–29%) in the Qingyang profile (Liu et al., 1981). Miao et al. (1984) also recorded the palynological assemblage from the upper member of the Tongchuan Formation in the Guluo and Kongyu outcrops in Hongdong, Shanxi Province, North China, located in the southeastern Ordos Basin. The assemblage is dominated by fern spores (60.4%–78.0%) including *Punctatisporites* (42.8%–65.1%), *Calamospora* (4.0%–6.3%), and *Verrucosisporites* (2.0%–7.0%). The pollen (22.0%–39.6%) in the assemblage mainly comprises *Piceaepollenites* (7.0%–11.6%), *Chordasporites* (1.6%–8.7%), and *Psophosphaera* (2.5%–8.0%) (Miao et al., 1984). As the upper member of the Tongchuan Formation includes YC8 and YC7, researchers in the 1980s did not realize the palynological difference between the two members. Sun et al. (1995) reported that the Anisian-Ladinian palynological assemblage in the northern China

10.3389/feart.2022.1008707

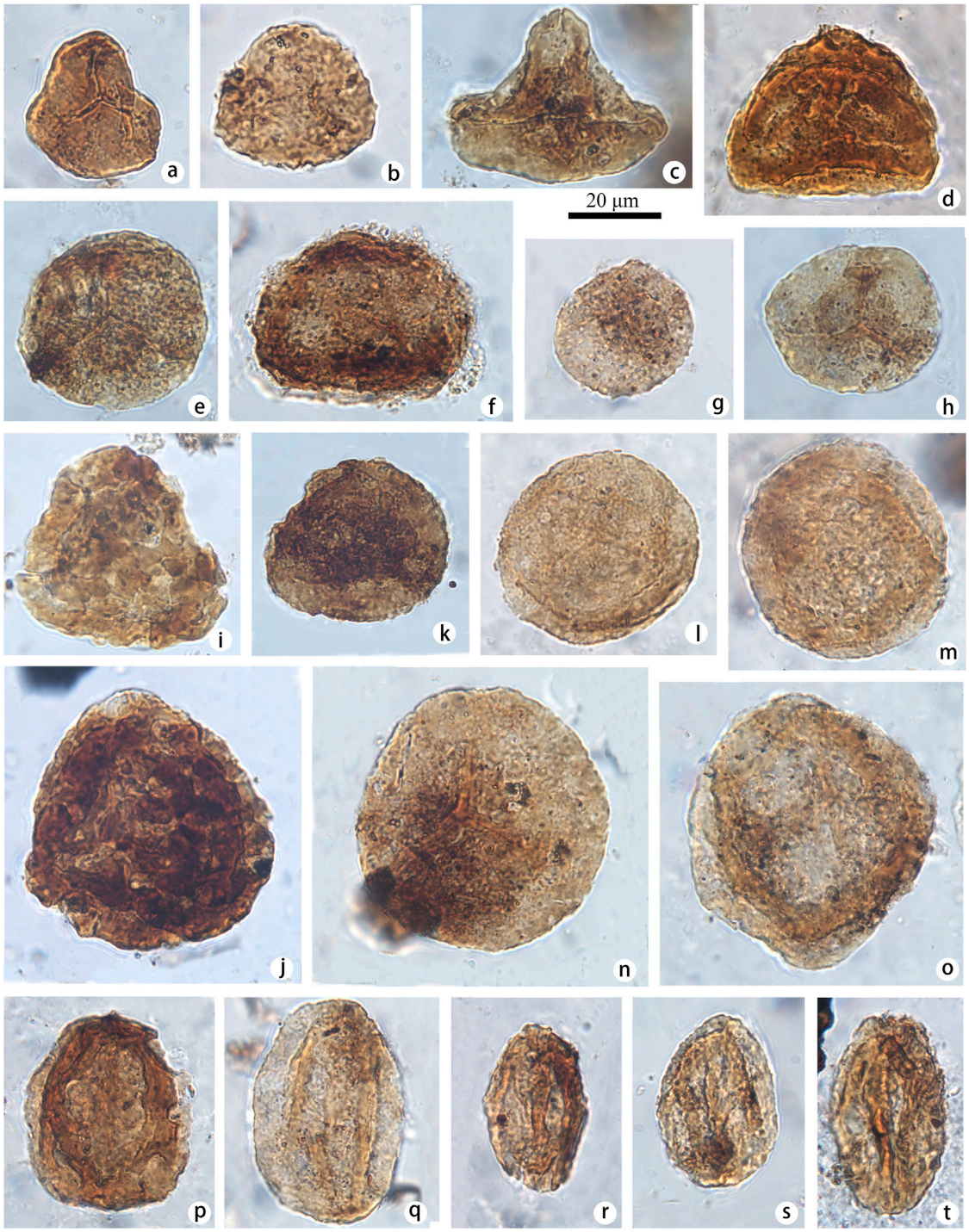

FIGURE 2
Selected spores and pollen identified at the Yunmeng profile (taxon name followed by sample number and position in England finder in parentheses). **(A)** *Cyathidites minor* (Couper, 1953) (a-STYM94, J11-2); **(B)** *Converrucosisporites decoratus* (Shang, 2011) (b-STYM48, R17-4); **(C)** *Dictyophyllidites harrisii* (Couper, 1958) (c-STYM48, N34-3); **(D)** *Duplexisporites rotundatus* (Shugaevskaya, 1969) (d-STYM01, N41-4); **(E)** *Verrucosisporites rotundus* (Singh, 1964) (e-STYM03, N23-3); **(F)** *Kraeuselisporites spinosus* (Jansonius, 1962) (f-STYM16, F20-1); **(G)** *Apiculatisporites bulliensis* (Helby et De Jersey, 1972) (g-STYM94, R8-3); **(H)** *Lundbladispora playfordi* (Balme, 1963) (h-STYM12, I26-1); **(I)** *Asseretospora gyrata* (Playford et Dettmann) (Schuurman, 1977) (i-STYM16, B21-4); **(J)** *Asseretospora curvata* (Qu, 1980) (j-STYM28, J12-2); **(K)** *Lundbladispora watangensis* (Qu, 1984) (k-STYM12, R36-2); **(L, M)** *Lundbladispora subornata* (Ouyang and Li, 1980) (l-STYM01, O45-2; m-STYM01, U25-4); **(N)** *Lundbladispora communis* (Ouyang and Li, 1980) (n-STYM94, K17-3); **(O)** *Lundbladispora* sp. (o-STYM01, M26-4); **(P)** *Aratrisporites exiguous* (Qu, 1984) (p-STYM28, M31-2); **(Q)** *Aratrisporites tenuispinosus* (Playford, 1965) (q-STYM01, N37-1); **(R)** *Aratrisporites coryliseminis* (Klaus, 1960) (r-STYM01, N37-1); **(S, T)** *Aratrisporites granulates* (Klaus) (Playford and Dettmann, 1965) (s-STYM21, R45-4, t-STYM01, T16-2).

10.3389/feart.2022.1008707

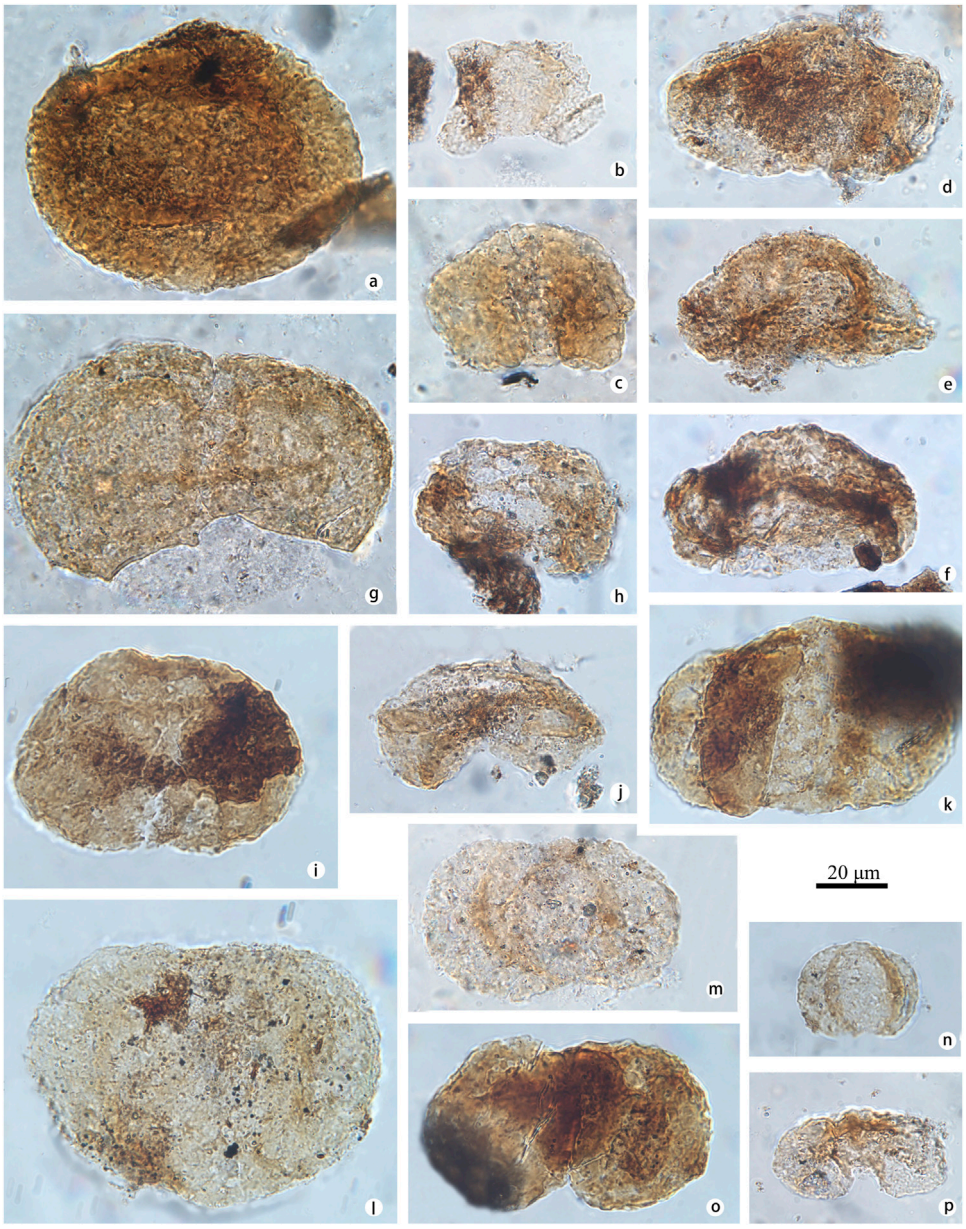

FIGURE 3
Selected pollen identified at the Yunmeng profile (taxon name followed by sample number and position in England finder in parentheses). **(A)** *Plicatipollenites indicus* (Lele, 1964) (a-STYM01, J46-3); **(B)** *Striatoabieites* sp. 1 (b-STYM21, L47-4); **(C)** *Striatoabieites brickii* (Sedova, 1956) (c-STYM01, L19-3); **(D–F)** *Striatoabieites duivenii* (Jansonius) (Hart, 1964), (d-STYM21, N41-3; e-STYM16, S14-1; f-STYM28, S23-1); **(G)** *Taeniaesporites combinatus* (Qu and Wang, 1990) (g-STYM01, M18-4); **(H)** *Taeniaesporites albertae* (Jansonius, 1962) (h-STYM28, F39-1); **(I)** *Taeniaesporites junior* (Klaus, 1960) Wu, 1982 (i-STYM88, A42-1); **(J)** *Taeniaesporites leptocorpus* (Qu, 1984) (j-STYM21, L45-1); **(K)** *Protohaploxypinus samoilovichii* (Jansonius) (Hart, 1964) (k-STYM48, T13-3); **(L)** *Protopinus subluteus* Bolkh, 1956 (l-STYM21, O34-4); **(M)** *Alisporites nuthallensis* (Clarke, 1965) (m-STYM01, K28-4); **(N)** *Alisporites parvus* (De Jersey, 1962) (n-STYM82, E21-4); **(O)** *Platysaccus luteus* (Bolkh.) (Li and Shang, 1980) (o-STYM88, I41-3); **(P)** *Platysaccus queenslundi* (De Jersey, 1962) (p-STYM21, L44-2).

palynofloristic realm could not be divided into two sub-assemblages according to their sporo-pollen sampling horizons and named the *Punctatisporites–Aratrisporites–Taeniaesporites–Parataeniaesporites* assemblages for both the Ermaying and Tongchuan formations in the Ordos Basin (Sun et al., 1995). Furthermore, the spores in the Yongping and Wayaobu formations (equivalent to members YC7 to YC1) on the Tuweihe profile in the northern Ordos Basin accounted for 56.2%–61.5% of the total grains (Wang et al., 2003). Therefore, it seems difficult to determine whether the palynological characteristics of the YC7 member are related to the lower layers (from YC8 to YC10) or upper member (from YC6 to YC1).

Finally, based on the samples from 12 boreholes (including X17, X30, X36, X40, X43, and X44) in the Ordos Basin, located 136 km westward of the Yunmeng profile, the palynological assemblages for the YC8 and YC7 members were separated and named *Aratrisporites–Punctatisporites* and *Asseretospora–Walchiites*, respectively (Ji and Meng, 2006). The *Aratrisporites–Punctatisporites*

10.3389/feart.2022.1008707

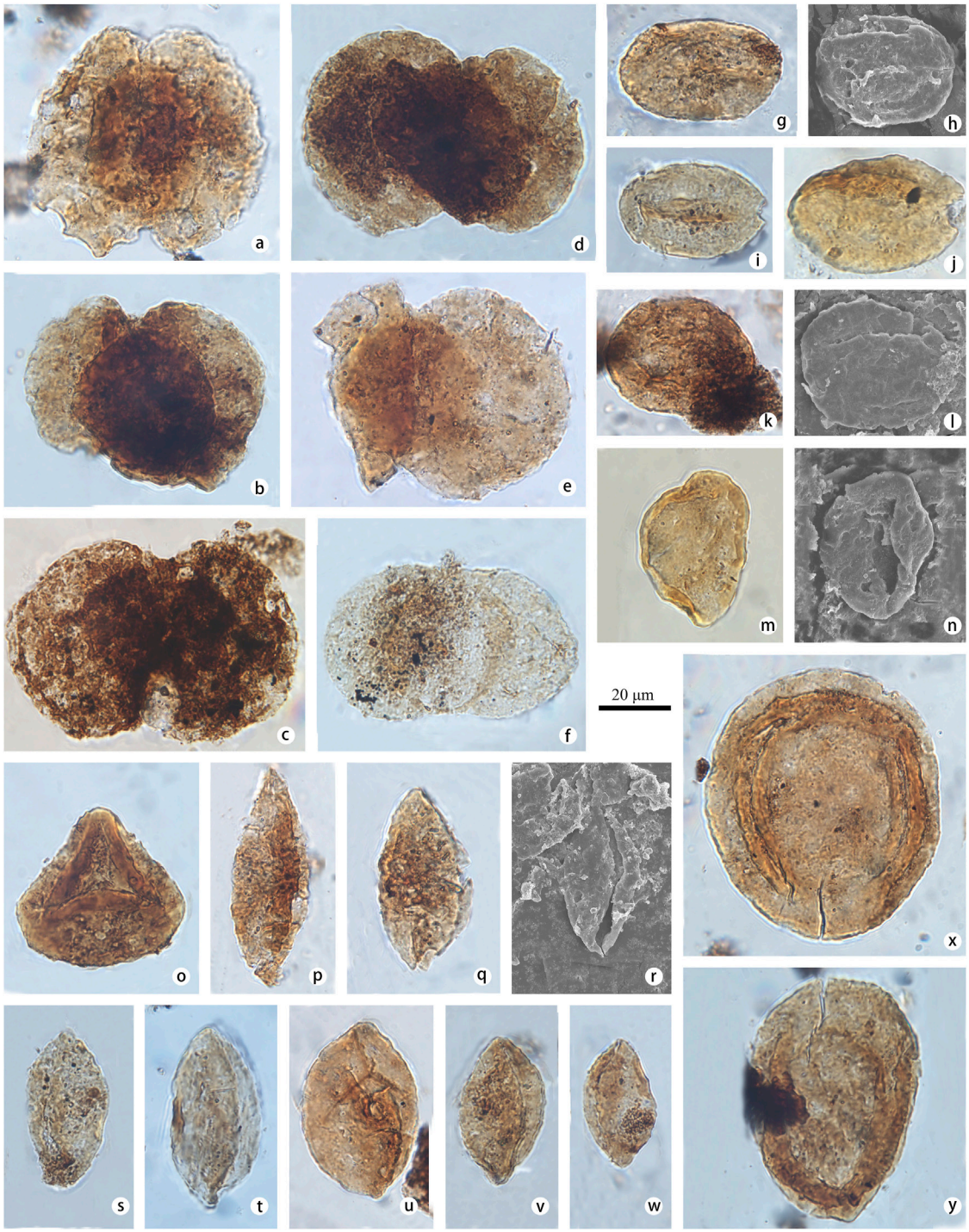

FIGURE 4
Selected pollen identified at the Yunmeng profile (taxon name is followed by sample number and position in England finder or stub number in parentheses). **(A)** *Podocarpidites paulus* (Bolkh.) (Xu and Zhang, 1980) (a-STYM16, P7-2); **(B, C)** *Podocarpidites ornatus* (Pocock, 1962) (b-STYM94, M34-4; c-STYM97, M34-1); **(D, E)** *Podocarpidites unicus* (Bolkh.) (Pocock, 1970) (d-STYM-88, N35-2; e-STYM16, R42-1); **(F)** *Podocarpidites multicinus* (Bolkh.) (Pocock, 1970) (f-STYM30, I29-4); **(G–J)** *Ovalipollis ovalis* (Krutzsch, 1955) (g, h-STYM01, O23-1, Stub-01; i-STYM26, P36-1; j-STYM01, N33-1); **(K, L)** *Ovalipollis breviformis* (Krutzsch, 1955) (k, l-STYM21, Q37-3, Stub-21); **(M, N)** *Chasmatosporites apertus* (Rogalska) (Nilsson, 1958) (m, n-STYM12, T20-3, Stub-12); **(O)** *Duplicisporites granulatus* (Leschik, 1955) (o-STYM94, L37-4); **(P–R)** *Cycadopites typicus* (Maljavkina) (Pocock, 1970) (p-STYM48, D46-1; q, r-STYM16, T23-2, Stub-16); **(S)** *Cycadopites adjectus* (De Jersey, 1964) (s-STYM27, I34-2); **(T)** *Cycadopites tivoliensis* (De Jersey, 1971) (t-STYM28, M47-4); **(U–W)** *Ginkgocycadophytus* spp. (u-STYM74, R34-1; v-STYM97, J31-2; w-STYM90, P16-2); **(X, Y)** *Discisporites* spp. (x-STYM74, D44-2; y-STYM94, G38-2).

assemblage is characterized by abundant fern spores (52.5%–88.7%), including *Aratrisporites* (6.8%–66.2%), *Punctatisporites* (4.0%–50.4%), *Osmundacidites* (3.5%–25.6%), *Verrucosisporites* (2.3%–18.0%), and gymnosperm pollen (11.3%–45.7%) represented by *Alisporites* (4.0%–14.1%), *Abietineaepollenites* (4.8%–10.2%), *Pinuspollenites* + *Piceaepollenites* (2.2%–13.3%), *Walchiites* (2.2%–12.0%), and

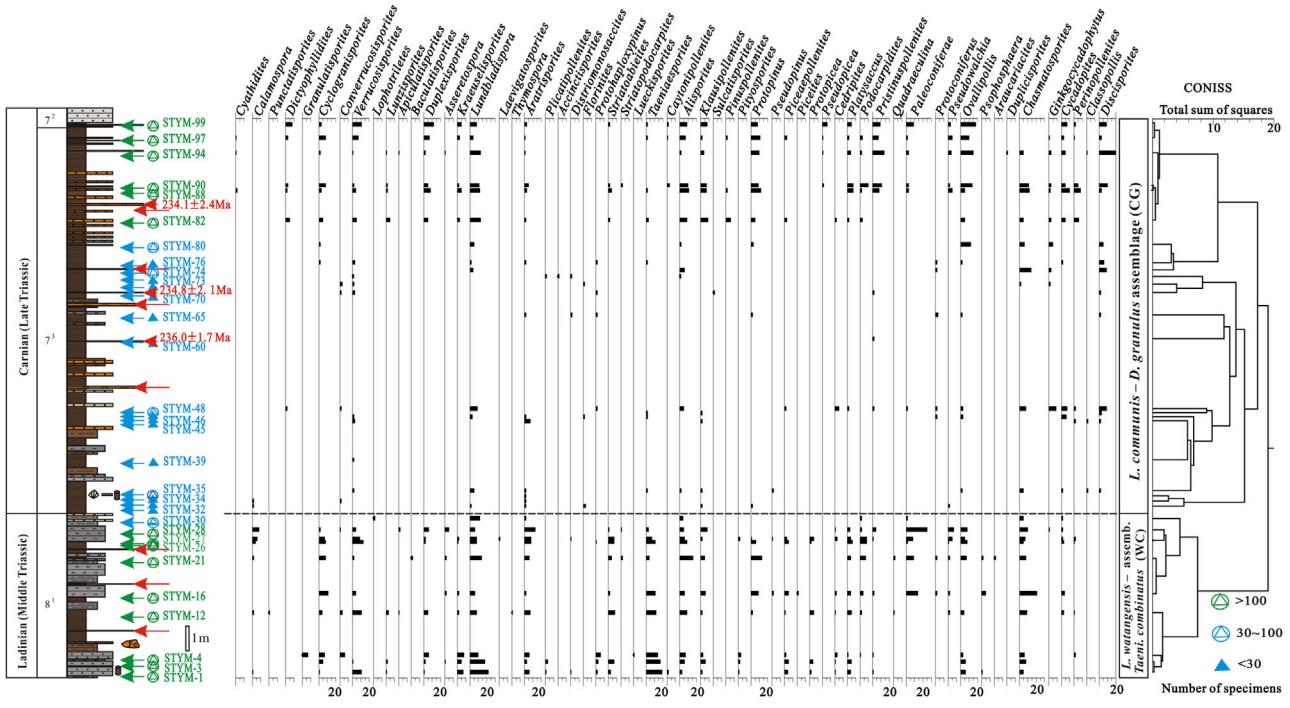

FIGURE 5
Stratigraphy, lithology, productive sample position, and relative sporo-pollen abundances at the Yunmeng profile, Ordos Basin, China.

Cycadopites (1.0%–6.0%). The *Asseretospora–Walchiites* assemblage comprises fern spores (15.9%–44.7%) represented by *Asseretospora* (5.2%–20.2%) and *Aratrisporites* (4.0%–15.8%), and gymnosperm pollen (53.3%–84.1%) including *Abietineaepollenites* + *Pinuspollenites* (8.4%–34.0%), *Walchiites* (4.0%–22.2%), and *Alisporites* (4.7%–15.6%).

The present WC and CG assemblages are comparable to the *Aratrisporites–Punctatisporites* and *Asseretospora–Walchiites* assemblages, respectively. The WC assemblage from the YC8-1 sub-member (i.e., the upper part of YC8 member) is part of the *Aratrisporites–Punctatisporites* assemblage from the whole YC8 member, while the CG assemblage from the YC7-3 sub-member (the lower part of the YC7 member) is part of the *Asseretospora–Walchiites* assemblage. This enables researchers to see all characteristics and the details of the palynological transition from the uppermost Ladinian to the lowest Carnian. The percentage of spores decreases from the YC8 to YC7, with an obvious excursion at the boundary between YC8 and YC7. While this might result from the withdrawal of lake shore vegetation accompanying the lake's widening and deepening, the number of spore species decreased greatly, especially *Lundbladispora* and *Aratrisporites*. Deng et al. (2018) summarized the palynological assemblages of the Yanchang Formation (*sensu lato*) in the Ordos Basin, named the *Asseretospora–Apiculatisporis–Chordasporites* (YC1–YC6) assemblage and *Punctatisporites–Aratrisporites–Verrucosisporites* (YC7–YC10) assemblage. Spore abundance varied between 30% and 70% in each, and, in many outcrops, the *Aratrisporites* content was as high *Punctatisporites* and *Verrucosisporites* in the *Punctatisporites–Aratrisporites–Verrucosisporites* assemblage, including the Qishuihe profile (Deng et al., 2018).

Three palynological assemblage zones were recently recognized based on 11 samples from the Triassic Tanzhuang and Anyao formations in the Jiyuan Basin (which might comprise the Ordos Basin), Henan Province, China—named the *Paleoconiferus–Cyclogranisporites–Rotundipollis*, *Cyclogranisporites–Osmundacidites–Punctatisporites*, and *Pseudopicea–Paleoconiferus–Protoconiferus* assemblage zones (in ascending order) (Lu et al., 2021). The first and last assemblages were dominated by gymnosperm pollen (52.3% and 47.6%, respectively) represented by *Paleoconiferus* and *Pseudopicea*, with fern spores mainly including *Cyclogranisporites*, *Osmundacidites*, and *Punctatisporites*. However, the second assemblage was dominated by algae (56.5%), fern spores (33.3%), and gymnosperm pollen (10.2%). This was also observed in the present WC and CG assemblages, which were dominated by gymnosperm pollen, along with algae at the horizon of the CG assemblage.

5 Discussion

5.1 Geological age

5.1.1 Isotopic dating

Although the geological age of YC7-3 on the Yunmeng profile is assigned to the Carnian based on U-Pb isotopic dating of three continuous rhyolitic tuff layers and ages 236.0 ± 1.7 Ma, 234.8 ± 2.1 Ma, and 234.1 ± 2.4 Ma have been obtained in ascending order (Sun et al., 2020), the latest isotopic dating near the Yunmeng profile showed the ages to be much older (240.9 ± 0.9 Ma for the detrital zircons from the tuffaceous sandstone in Mazhuang; Zhao et al., 2020). The old

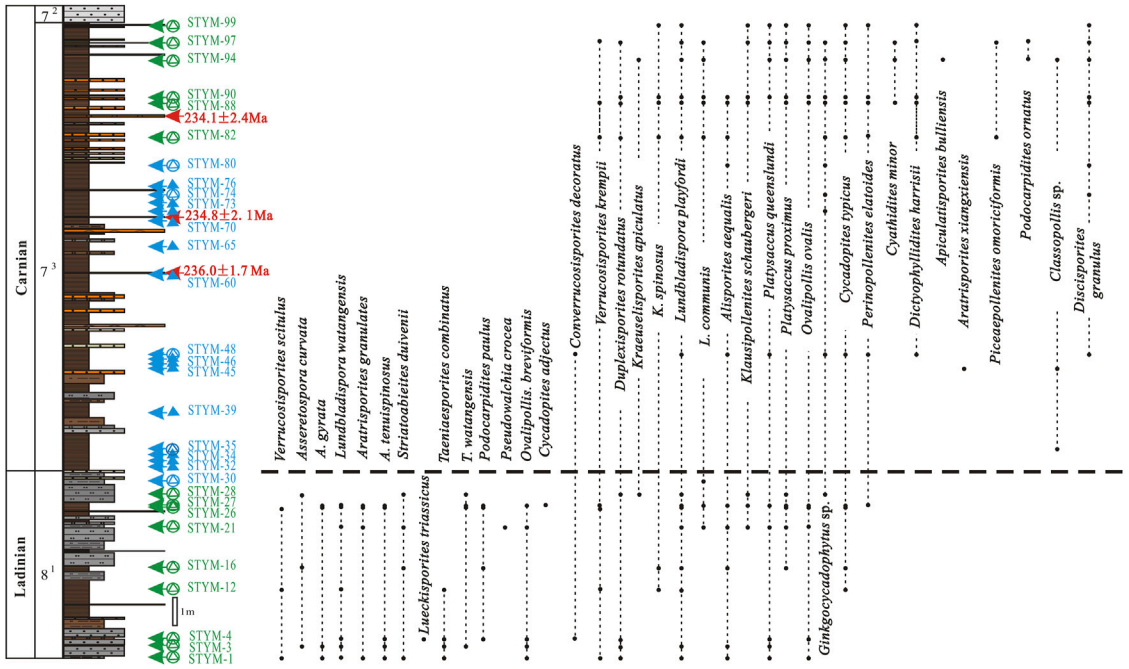

FIGURE 6
Distribution of selected palynological taxa during the Ladinian–Carnian transition in the Yunmeng profile, Ordos Basin, China.

group of detrital zircons could not be regarded as of eruptive and depositional ages (Fedo et al., 2003), and they were also detected as inherited zircons in sample STYMD-62 (Sun et al., 2020). Some inherited zircons were dated older in the Yunmeng profile; however, considering the number of concording zircons and the stratigraphic sequence, the isotopic dating results indicated that YC7 in Ordos Basin was deposited at 234.1–236.0 Ma (Sun et al., 2020).

5.1.2 Palynological biostratigraphy

Unlike in South China and Europe, the Triassic successions in the Ordos Basin are terrestrial without any marine interlayers; therefore, palynology is one of the major fossils indexes used for stratigraphic correlation (Liu et al., 1981; Shang, 2011). At the GSSP section of the Carnian, the palynological criteria of the basal Carnian are the first observations of *Vallasporites ignacii*, *Patinasporites densus,* and *Aulisporites* cf. *A. astigmosus*, together with *Duplicisporites verrucosus* and *Camerosporites secatus*, "*Lueckisporites*" cf. *singhii*, which are auxiliary indicators of the Carnian (Mietto et al., 2012). Because the GSSP of the Carnian is indicated by *Daxatina canadensis*, it is lower than the traditional base of the Carnian (including Cordevolian, Julian, and Tuvalian) in the Alps and circum-Tethys area, which was marked by the *Trachyceras aon* zone (Visscher and Brugman, 1981). Meanwhile, *C. secatus* was recorded in Yunnan and Guizhou, China, where the bases of the palynomorph-bearing strata are Carnian-aged marine limestones, as evidenced by the presence of conodonts (*Neogondolella polygnathiformis* zone; Yang et al., 1995). Thus, this praecolpate pollen, together with other palynomorphs in the Banan and Sanqiao formations in Guizhou Province, China, are late Tuvalian in age (Shang, 2011). The present WC and CG assemblages in the Yunmeng profile in the Ordos Basin shared 17 known species with those in the Banan and Sanqiao formations, Guizhou Province, China, including *Calamospora nathorstii*, *C. padata*, *Punctatisporites crassexinis*, *Dictyophyllidites harrisii*, *Verrucosisporites congestus*, *V. morulae*, *Lundbladispora playfordi*, *Aratrisporites scabratus*, *Lueckisporites triassicus*, *Taeniaesporites albertae*, *T. junior*, *T. leptocorpus*, *Klausipollenites decipiens*, *Platysaccus proximus*, *P. queenslandi*, *Ovalipollis ovalis,* and *Cycadopites tivoliensis*. In addition to these species, 22 have been recorded in Late Triassic deposits in Eurasia, South America, North America, Australia, and Antarctica (Halle, 1908; Couper, 1953; Couper, 1958; Leschik, 1955; Nilsson, 1958; Klaus, 1960; De Jersey, 1962; De Jersey, 1964; De Jersey, 1972; Bharadwaj et Singh, 1964; Mädler, 1964; Clarke, 1965; Gair et al., 1965; Playford, 1965; Playford and Dettmann, 1965; Scheuring, 1970; Arjang, 1975; Fisher and Bujak, 1975; Schuurman, 1977): *Cyathidites minor*, *Verrucosisporites krempii*, *V. remyanus*, *Lunzisporites lunzensis*, *L. sparsus*, *Asseretospora gyrate*, *Aratisporites coryliseminis*, *A. granulates*, *A. coryliseminis*, *A. strigosus*, *A. tenuispinosus*, *A. aequalis*, *A. circulicorpus*, *A. nuthallensis*, *A. parvus, Ovalipollis grebeae*, *O. minimus*, *Duplicisporites granulatus*, *Chasmatosporites apertus*, *Cycadopites adjectus*, *C. reticulatus*, and *Perinopollenites elatoides*. However, six species—including *Cyclogranisporites multigranus*, *Apiculatisporis bulliensis*, *Kraeuselisporites apiculatus*, *K. spinosus*, *Plicatipollenites indicus*, and *K. schaubergeri*—from the Permian or even the Carboniferous of France, England, Canada, Australia, and India (Potonie and Klaus, 1954; Jansonius, 1962; Lele, 1964; Smith and Butterworth, 1967) have also been recorded in the Triassic of South and North China (Song et al., 2000; Ouyang et al., 2011; Ji et al., 2015; Ji et al., 2017; Liu et al., 2015). Moreover, 18 species from the Jurassic–Cretaceous or Paleogene from Canada and Siberia—*Converrucosisporites saskatchewanensis*, *Verrucosisporites asymmetricus, V. rotundus, Duplexisporites rotundatus*, *Alisporites bilateralis, A. rotundus*, *Protopinus subluteus, Piceaepollenites omoriciformis, Platysaccus luteus*, *Podocarpidites multicinus*, *P. ornatus*, *P. paulus*, *P. unicus*, *Pseudowalchia crocea*,

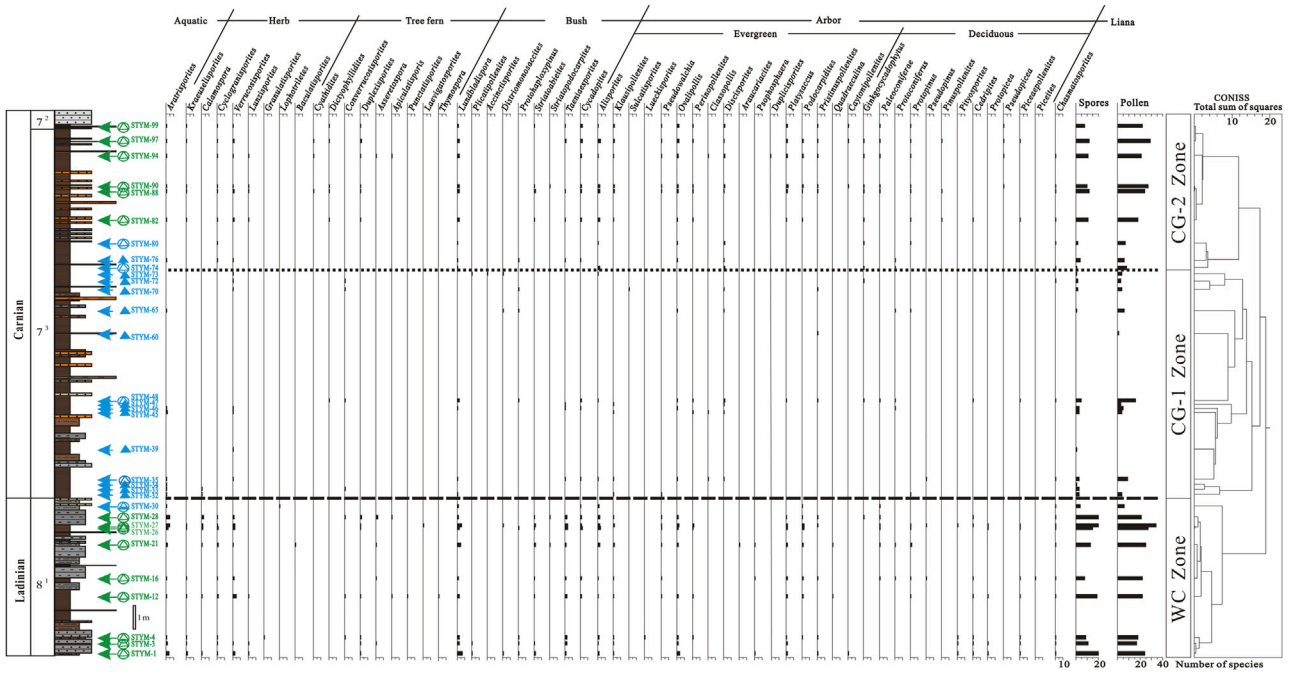

FIGURE 7
Diversity and reconstructed living habit of palynofloras at the Yunmeng profile, Ordos Basin, China.

Ovalipollis breviformis, *Psophosphaera cognatus*, *Araucariacites australis*, and *Cycadopites typicus* (Cookson, 1947; Malyavkina, 1949; Krutzsch, 1955; Bolkhovitina, 1956; Rouse, 1959; Pocock, 1962; Pocock, 1970; Singh, 1964; Shugaevskaya, 1969)—were found in the present assemblages; however, most of them have also been reported in other Triassic palynological assemblages worldwide (Varyukhina, 1961; Clarke, 1965; Scheuring, 1966; Schulz, 1967; Pocock, 1970; Warrington, 1970; Gradstein, 1971; Planderova, 1972; Horowitz, 1973; Tuzhikova, 1975; 1979; Kimyai, 1977; Tuzhikova, 1980; Semenova, 1987; Song et al., 2000). Another 20 local species, including *Cyclogranisporites callosus*, *Converrucosisporites decorates*, *Verrucosisporites mimicus, V. scitulus*, *Apiculatisporis pilosus, Baculatisporites versiformis, Asseretospora curvata, L. communis*, *L. microreticuIata*, *L. minuta*, *L. sinica*, *L. subornata*, *L. watangensis*, *Aratrisporites exiguous, Arat. xiangxiensis*, *Taeniaesporites combinatus*, *T. divisus, T. watangensis*, *Podocarpidites transverses,* and *D. granulus,* have been recorded in the Triassic or early Jurassic in China, especially in the Ordos Basin (Ouyang, 1982; Miao et al., 1984; Zhang, 1984; Song et al., 2000). Therefore, the overall geological age of the present palynoflora is around the Carnian.

The CG assemblage from YC7-3 was considered to be Late Triassic Carnian in age because, around the world, the species *Cyathidites minor* (Couper, 1953), *Dictyophyllidites harrisii* (Couper, 1958), *Apiculatisporis bulliensis* (Helby ex De Jersey, 1971), *Aratrisporites xiangxiensis* (Li and Shang, 1980), *Piceaepollenites omoriciformis* (Bolkh.) (Xu and Zhang, 1980), *Podocarpidites ornatus* (Pocock, 1962), and *Discisporites granulus* (Zhang, 1984), and genus *Classopollis* (Pflug, 1953) were only found in the CG assemblage and were never aged older than the Carnian of the Late Triassic (Figure 6).

Meanwhile, some of the species in the WC assemblage, including *Lundbladispora nejburgii* (Schulz, 1964), *Plicatipollenites indicus* (Lele, 1964), *Striatoabieites bricki* (Sedova, 1956), *S. duivenii* (Jansonius) (Hart, 1964), and *Klausipollenites schaubergeri* (Potonie et Klaus) (Jansonius, 1962) are normally found in the Lower Triassic and the Anisian in Eurasia (Geiger and Hopping 1968; Sakulina, 1973; Vinogradova, 1974; Tuzhikova, 1975; Warrington, 1979). Some local species, such as *Cyclogranisporites callosus* (Du, 1985), *Verrucosisporites mimicus* (Qu and Wang, 1986), *Lundbladispora communis* (Ouyang and Li, 1980), *L. microreticulata* (Qu, 1982), *L. minuta* (Qu, 1984), *Lundbladispora sinica* (Ouyang and Li, 1980), *Lundbladispora subornata* (Ouyang and Li, 1980), *L. watangensis* (Qu, 1984), *Aratrisporites exiguous* (Qu, 1984), *Taeniaesporites combinatus* (Qu and Wang, 1990), *Taeniaesporites divisus* (Qu, 1982), and *Taeniaesporites watangensis* (Qu, 1984) were reported in the Lower Triassic and never in the Upper Triassic in China. Thus, the age of the WC assemblage from YC8-1 was assigned to the Middle Triassic Ladinian (Figure 6).

5.2 Reconstructed palynofloras

Based on the compositions, habitats, and vertical distributions of the mother plants of pollen and spores, three palynofloras were reconstructed on the Yunmeng profile in Ordos Basin, China (Figure 7).

5.2.1 Latest Ladinian palynoflora

The latest Ladinian palynoflora reconstructed from the YC8-1 sub-member on the Yunmeng profile in the Ordos Basin can be represented by the *L. watangensis–T. combinatus* assemblage (WC). It is quite diverse in its composition, comprising 121 species of 47 genera (Supplementary Appendix S1). The spores in this palynoflora include 54 species belonging to 17 genera. The most diverse genera were *Verrucosisporites* (10 species), *Lundbladispora* (10), and *Aratrisporites* (8), which accounted for half of the spore species. The botanical affinity of *Verrucosisporites* spores might be with those of lycophytes (Isoetales) or Pteridophytes (Zygopteridales, Botryopteridales, and

Marattiales) (Mamay, 1950; Balme, 1995; Taylor et al., 2009); however, *Bromsgrovia* with *in situ Verrucosisporites* spores from the Anisian in the United Kingdom are considered horsetails (Seyfullah et al., 2013). Therefore, the *Verrucosisporites* in the present flora are considered sphenophytes, an emerging plant on the Triassic Ordos Lake shore. *Lundbladispora* spores belong to Pleuromeiales, lycophytes (Balme, 1995), and are recorded *in situ* in the Devonian lycopod strobill *Bisporangiostrobus* (Chitaley and McGregor, 1988) and Triassic *Pleuromeia sternbergii* (Grauvogel-Stamm and Lugardon, 2004). As the remarkable characteristic of three rounded papillae between the trilete rays on the proximal surface is found in the Triassic *Pleuromeia* cone, we agree that the mature microspores of *P. sternbergii* are *Lundbladispora*-type (Balme, 1995). *Aratrisporites* spores are additional lycophytic microspores that have been reported *in situ* in *Annalepis zeilleri*, *Araucarites tomiensis*, *Cyclostrobus sydneyensis*, *Lycostrobus scottii*, *Tomiostrobus radiates,* and *Isoetes ermayingense* (Wang, 1991; Balme, 1995) and are considered quillwort and an aquatic lycopod (Retallack, 1997). Sphenophytes include *Calamospora*, *Cyclogranisporites*; lycophytes, *Kraeuselisporites*; and pteridophytes, *Lunzisporites*, *Punctatisporites*, *Granulatisporites*, *Lophotriletes*, *Baculatisporites*, *Apiculatisporis*, *Duplexisporites*, *Asseretospora*, *Laevigatosporites,* and *Thymospora*. These are herbs or fern trees surrounding the lake and riverside or distributed on the wet lowland.

The pollen of the latest Ladinian palynoflora mainly comprises Pteridospermophytes: *Taeniaesporites* (seven species), *Alisporites* (seven), coniferophytes: *Podocarpidites* (five), *Ovalipollis* (five), and cycadophytes: *Cycadopites* (five species). *Taeniaesporites* and *Alisporites* have bisaccate pollen with or without striae on the corpus and are considered *Permotheca disparis*-type pollen because of their morphological similarity to *in situ P. disparis* (Zalessky) Naugolnykh pollen (Krassilov et al., 1999; Zhang J. G. et al., 2021). They might have been evergreen peltaspermale shrubs. *Ovalipollis* (Krutzsch) Klaus is an elliptical protobisaccate pollen with anasulcus being regarded as *Majonica alpina*-type (Zhang J. G. et al., 2021) and might be an evergreen tree of Voltziales. The mother plants yielding *Podocarpidites* pollen should be Podocarpaceae arbors in the dry lowlands and uplands as canopy forests (Li et al., 2020). *Cycadopites* are heliophyte shrubs present in the lowlands (Mander et al., 2010; Paterson et al., 2016). These five gymnosperm pollen genera might represent the leading taxa in lowland and upland vegetation. Other diverse pollen species included coniferophytes: *Platysaccus* (four species) and Pteridospermophytes: *Klausipollenites* (three) and *Striatoabieites* (three), which are evergreen trees and shrubs. Compared to evergreen plants, deciduous arbor conifer trees are diverse at the genus level but impoverished at the species level: *Protopinus*, *Pseudopinus*, *Cedripites*, *Piceaepollenites*, *Piceites*, *Protopicea,* and *Pseudopicea*. They may have been present in the upland or mountainous areas.

In summary, the latest Ladinian palynoflora are diverse in every niche, including lakes, bogs, rivers, wet and dry lowlands, uplands, and mountainous peaks. The lacustrine vegetation is characterized by aquatic *Aratrisporites* quillworts, *Verrucosisporites*, and *Calamospora* sphenopsids as emerging plants on the shore. The wet lowland vegetation mainly comprises *Lundbladispora* lycopods on the riverbank, *Verrucosisporites* (*Kraeuselisporites* sphenopsids), and some herbaceous ferns such as *Lunzisporites*, *Apiculatisporis,* and *Asseretospora*. The dry lowland vegetation is characterized by evergreen *Cycadopites*, *Taeniaesporites* bushes, and *Duplexisporites–Asseretospora* fern trees. The upland vegetation consists of diverse evergreen arbor forests represented by *Alisporites*, *Ovalipollis*, *Platysaccus,* and *Podocarpidites* mingled with deciduous conifer trees such as *Cedripites* and *Piceaepollenites* on the high mountains.

5.2.2 Earliest Carnian palynoflora

The earliest Carnian palynoflora reconstructed from the lower part of the YC7-3 sub-member on the Yunmeng profile in Ordos Basin can be represented by the early sub-assemblage of the *L. communis–D. granulus* assemblage (CG-1). This comprises 35 species of 29 genera, which is small not only in the number of species but also in the quantity of specimens compared to the latest Ladinian palynoflora (Supplementary Appendix S1; Figure 7). The spores in this small palynoflora include only nine species of six genera: *Lundbladispora* (three species), *Converrucosisporites* (two), *Aratrisporites*, *Calamospora*, *Verrucosisporites*, and *Dictyophyllidites*. Gymnosperm pollen (26 species of 23 genera) are relatively diverse at the genus level, including Pteridospermophytes (*Protohaploxypinus*, *Taeniaesporites*, *Alisporites, Klausipollenites*, *Sulcatisporites*), Coniferophytes (*Plicatipollenites*, *Accinctisporites*, *Protohaploxypinus*, *Pseudowalchia*, *Ovalipollis*, *Paleoconiferae*, *Protoconiferus*, *Pristinuspollenites*, *Protopinus*, *Pseudopinus*, *Cedripites*, and *Piceaepollenites*), Cycadophytes (*Cycadopites*), and Ginkgophytes (*Ginkgocycadophytus*).

Although it is small, the earliest Carnian palynoflora covers most niches, including lakes, rivers, wet and dry lowlands, uplands, and mountains. The lacustrine vegetation comprises aquatic *Aratrisporites* quillworts and *Verrucosisporites–Calamospora* sphenopsids as emerging plants on the shore. The wet lowland vegetation consists of *Lundbladispora* lycopods on the riverbank and some fern trees represented by *Dictyophyllidites* and *Converrucosisporites*. The dry lowland vegetation is characterized by evergreen *Cycadopites* bushes and Pteridospermophytes shrubs such as *Taeniaesporites* and *Protohaploxypinus*, as well as evergreen voltzialean shrubs such as *Plicatipollenites* and *Accinctisporites*. The upland vegetation consists of evergreen arbor forests represented by *Alisporites*, *Klausipollenites*, *Pseudowalchia*, *Ovalipollis*, *Platysaccus,* and *Pristinuspollenites* mingled with deciduous conifer trees such as *Cedripites* and *Piceaepollenites* on the high mountains. The most conspicuous characteristic of upland vegetation is the acceding of Cheirolepidiaceae and Cupressaceae evergreen scaly leaf trees represented by *Discisporites* and *Perinopollenites*, respectively. This indicates that the two coniferous families most likely originated in the early Carnian (Taylor et al., 2009).

5.2.3 Early Carnian palynoflora

The early Carnian palynoflora reconstructed from the upper part of the YC7-3 sub-member on the Yunmeng profile in Ordos Basin can be represented by the late sub-assemblage of the *L. communis–D. granulus* assemblage (CG-2). It comprises 61 species belonging to 37 genera, which is much more diverse than the earliest Carnian palynoflora (Figure 7). The spores in this palynoflora comprise 16 species belonging to 11 genera, including *Lundbladispora* (three species), *Verrucosisporites* (two), *Duplexisporites* (two), *Aratrisporites*, *Kraeuselisporites, Cyclogranisporites, Lunzisporites*, *Cyathidites, Dictyophyllidites, Asseretospora,* and *Apiculatisporis*. The gymnosperm pollen (45 species in 26 genera) is quite diverse, especially comprising *Cycadopites* (five species), *Alisporites* (five), *Taeniaesporites* (three), *Ovalipollis* (three), *Platysaccus* (three), and *Podocarpidites* (three species).

TABLE 2 Botanical affinities, habits, eco-groups, and environments of dispersed palynofloras in Ordos Basin, China.

Taxon	Infraturma	Botanical affinity	Habit	SEG	Environment
Aratrisporites	Monolete	Lycophytes: Isoetales	Aquatic	Aquatic	Hygrophytic
Lundbladispora	Trilete	Lycophytes: Pleuromeiales	Woody bush	Dry lowland	Hydrophytic D
Kraeuselisporites	Trilete	Lycophytes: Sellaginellales	Herbaceous	Wet lowland	Hydrophytic B
Calamospora	Trilete	Sphenophytes: Equisetales	Herbaceous	Lacustrine shore	Hydrophytic A
Cyclogranisporites	Trilete	Sphenophytes: Equisetales	Herbaceous	Lacustrine shore	Hydrophytic A
Verrucosisporites	Trilete	Sphenophytes: Equisetales	Herbaceous	Lacustrine shore	Hydrophytic A
Lunzisporites	Trilete	Sphenophytes: Equisetales	Herbaceous	Wet lowland	Hydrophytic B
Granulatisporites	Trilete	Pteridophytes: Botryopteridales	Herbaceous	Wet lowland	Hydrophytic B
Lophotriletes	Trilete	Pteridophytes: Botryopteridales	Herbaceous	Wet lowland	Hydrophytic B
Baculatisporites	Trilete	Pteridophytes: Osmundaceae	Herbaceous	Wet lowland	Hydrophytic B
Cyathidites	Trilete	Pteridophytes: Cyatheaceae	Fern tree	Wet lowland	Hydrophytic C
Dictyophyllidites	Trilete	Pteridophytes: Dipteridaceae	Fern tree	Wet lowland	Hydrophytic C
Converrucosisporites	Trilete	Pteridophytes: Dipteridaceae	Fern tree	Wet lowland	Hydrophytic C
Duplexisporites	Trilete	Pteridophytes: Dicksoniaceae	Fern tree	Wet lowland	Hydrophytic C
Asseretospora	Trilete	Pteridophytes: Pteridaceae	Fern tree	Wet lowland	Hydrophytic C
Apiculatisporites	Trilete	Pteridophytes: Marattiales	Fern tree	Wet lowland	Hydrophytic C
Punctatisporites	Trilete	Pteridophytes: Marattiales	Fern tree	Wet lowland	Hydrophytic C
Laevigatosporites	Monolete	Pteridophytes: Marattiales	Fern tree	Wet lowland	Hydrophytic C
Thymospora	Monolete	Pteridophytes: Marattiales	Fern tree	Wet lowland	Hydrophytic C
Plicatipollenites	Monosaccites	Voltziales: Utrechtiaceae	Evergreen shrub	Dry lowland	Xerophytic
Accinotisporites	Monosaccites	Voltziales: Utrechtiaceae	Evergreen shrub	Dry lowland	Xerophytic
Distriomonosaccites	Monosaccites	Voltziales: Utrechtiaceae	Evergreen shrub	Dry lowland	Xerophytic
Protohaploxypinus	Striatiti	Pteridospermophytes: Peltaspermales	Evergreen shrub	Dry lowland	Mesophytic
Striatoabieites	Striatiti	Pteridospermophytes: Peltaspermales	Evergreen shrub	Dry lowland	Mesophytic
Striatopodocarpites	Striatiti	Pteridospermophytes: Peltaspermales	Evergreen shrub	Dry lowland	Mesophytic
Taeniaesporites	Striatiti	Pteridospermophytes: Peltaspermales	Evergreen shrub	Dry lowland	Mesophytic
Cycadopites	Plicates	Cycadales	Evergreen shrub	Dry lowland	Mesophytic
Alisporites	Disaccites	Pteridospermophytes: Corystospermales	Evergreen arbor	Upland	Mesophytic
Klausipollenites	Disaccites	Pteridospermophytes: Corystospermales	Evergreen arbor	Upland	Mesophytic
Sulcatisporites	Disaccites	Pteridospermophytes: Corystospermales	Evergreen arbor	Upland	Mesophytic
Lueckisporites	Striatiti	Voltziales: Majoniaceae	Evergreen arbor	Upland	Mesophytic
Pseudowalchia	Disaccites	Voltziales	Evergreen arbor	Upland	Mesophytic
Ovalipollis	Saccites	Voltziales	Evergreen arbor	Upland	Mesophytic
Perinopollenites	Poroses	Coniferophytes: Cupressiaceae	Evergreen arbor	Upland	Xerophytic
Classopollis	Poroses	Coniferophytes: Cheirolepidiaceae	Evergreen arbor	Upland	Xerophytic
Discisporites	Poroses	Coniferophytes: Cheirolepidiaceae	Evergreen arbor	Upland	Xerophytic
Psophosphaera	Aletes	Coniferophytes: Araucariaceae?	Evergreen arbor	Upland	Mesophytic
Araucariacites	Aletes	Coniferophytes: Araucariaceae	Evergreen arbor	Upland	Mesophytic
Duplicisporites	Aletes	Coniferophytes: Araucariaceae?	Evergreen arbor	Upland	Mesophytic

(Continued on following page)

TABLE 2 (*Continued*) Botanical affinities, habits, eco-groups, and environments of dispersed palynofloras in Ordos Basin, China.

Taxon	Infraturma	Botanical affinity	Habit	SEG	Environment
Platysaccus	Disaccites	Coniferophytes: Podocarpaceae	Evergreen arbor	Upland	Mesophytic
Podocarpidites	Disaccites	Coniferophytes: Podocarpaceae	Evergreen arbor	Upland	Mesophytic
Pristinuspollenites	Disaccites	Coniferophytes: Podocarpaceae	Evergreen arbor	Upland	Mesophytic
Quadraeculina	Disaccites	Coniferophytes: Podocarpaceae	Evergreen arbor	Upland	Mesophytic
Caytonipollenites	Disaccites	Caytoniales	Evergreen arbor	Upland	Mesophytic
Ginkgocycadophytus	Plicates	Ginkgoales	Deciduous arbor	Upland	Xerophytic
Paleoconiferae	Disaccites	Coniferales	Deciduous arbor	Upland	Xerophytic
Protoconiferus	Disaccites	Coniferales	Deciduous arbor	Upland	Xerophytic
Protopinus	Disaccites	Coniferophytes: Pinaceae	Deciduous arbor	Upland	Xerophytic
Pseudopinus	Disaccites	Coniferophytes: Pinaceae	Deciduous arbor	Upland	Xerophytic
Pinuspollenites	Disaccites	Coniferophytes: Pinaceae	Deciduous arbor	Upland	Xerophytic
Pityosporites	Disaccites	Coniferophytes: Pinaceae	Deciduous arbor	Upland	Xerophytic
Cedripites	Disaccites	Coniferophytes: Pinaceae	Deciduous arbor	Upland	Xerophytic
Protopicea	Disaccites	Coniferophytes: Piceoidea	Deciduous arbor	Upland	Xerophytic
Pseudopicea	Disaccites	Coniferophytes: Piceoidea	Deciduous arbor	Upland	Xerophytic
Piceaepollenites	Disaccites	Coniferophytes: Piceoidea	Deciduous arbor	Upland	Xerophytic
Piceites	Disaccites	Coniferophytes: Piceoidea	Deciduous arbor	Upland	Xerophytic
Chasmatosporites	Plicates	Gnetales?	Liana		

The early Carnian palynoflora shows characteristics of recovery from the earliest Carnian palynoflora and adaptation to seasonal climate. Almost all niches are occupied by different kinds of plants. The lacustrine vegetation is represented by *Verrucosisporites–Cyclogranisporites* sphenopsids as emerging plants on the shore, as well as some aquatic *Aratrisporites* quillworts. The wet lowland vegetation includes abundant *Lundbladispora* lycopods on the riverbank and some fern trees, such as *Cyathidites*, *Dictyophyllidites*, *Duplexisporites*, *Asseretospora,* and *Apiculatisporis*. Dry lowland vegetation is characterized by evergreen *Cycadopites* bushes and Pteridospermophytes shrubs, such as *Taeniaesporites* and *Striatoabieites*. The upland vegetation consists of evergreen arbor forests represented by *Alisporites*, *Klausipollenites*, *Pseudowalchia*, *Ovalipollis*, *Discisporites*, *Platysaccus, Podocarpidites,* and *Pristinuspollenites* mingled with deciduous *Ginkgocycadophytus* and conifer trees such as *Protopinus* and *Pseudopicea* on the high mountains. The most conspicuous characteristic of the dry lowland vegetation is the disappearance of Utrechtiaceae evergreen conical leaf shrubs, which are seen in the earliest Carnian flora represented by *Plicatipollenites* and *Accinctisporites*; however, they are neither the main components in the latest Ladinian nor in the earliest Carnian palynofloras.

5.3 Climatic changes

5.3.1 Early and Middle Triassic climate

The Early and Middle Triassic climate in the Tethys area was arid in the tropical and subtropical areas (Parrish, 1993; Wilson et al., 1994; Kent and Olsen, 2000), with green vegetation present only along the permanent rivers (the gallery forests) (Shi et al., 2021). However, the arid climate periodically experienced humid pulses during the Early and Middle Triassic (Preto et al., 2010), and the middle and late Pelsonian humid events of the Anisian are well-documented by macroflora and palynoflora fossils Kustatscher and Van Konijnenburg-van Cittert, 2010). These humid pulses might have been important for climate change in the Ordos Basin as the changes caused the transition in the deposits from the magenta-red deposit of the Heshanggou Formation to the green and gray deposits with red interlayers of the Zhifang Formation (Qu, 1980). The disappearance of the reddish layers and the appearance of the coal seams indicate the beginning of the Yanchang Formation (*sensu lato*) (IGCAGS, 1980), which might be attributed to the Ladinian humid event marked by paleokarst breccia in the Dolomite Alps (Mutti and Weissert, 1995).

5.3.2 Carnian pluvial event

The Carnian pluvial event (CPE) is recognized as a carbonate crisis (Schlager and Schollnberger, 1974), reef crisis (Brandner, 1984; Donofrio., 1991; Ruttner et al., 1991), and black shale events (Hornung and Brandner, 2005) that occurred in the early Carnian epoch, in both the tropical Tethys and boreal areas (Dubiel et al., 1991; Shi et al., 2009; Preto et al., 2010; Wang et al., 2012; Mueller et al., 2015; Mueller et al., 2016). Since the CPE is also marked by negative carbon isotopic excursion (Dal Corso et al., 2012; Dal Corso et al., 2015), it is regarded as a global event caused by mega-monsoons (Dubiel et al., 1991; Mutti and Weissert, 1995) or increased atmospheric CO_2 from volcanic eruptions (Dal Corso et al., 2012; 2015; Mueller et al., 2016). The CPE is marked by a short-lived increase in rainfall (Preto and Hinnov, 2003; Hornung and Brandner, 2005; Rigo et al., 2007) in the Carnian. The vegetation changes in the western Tethys during the CPE

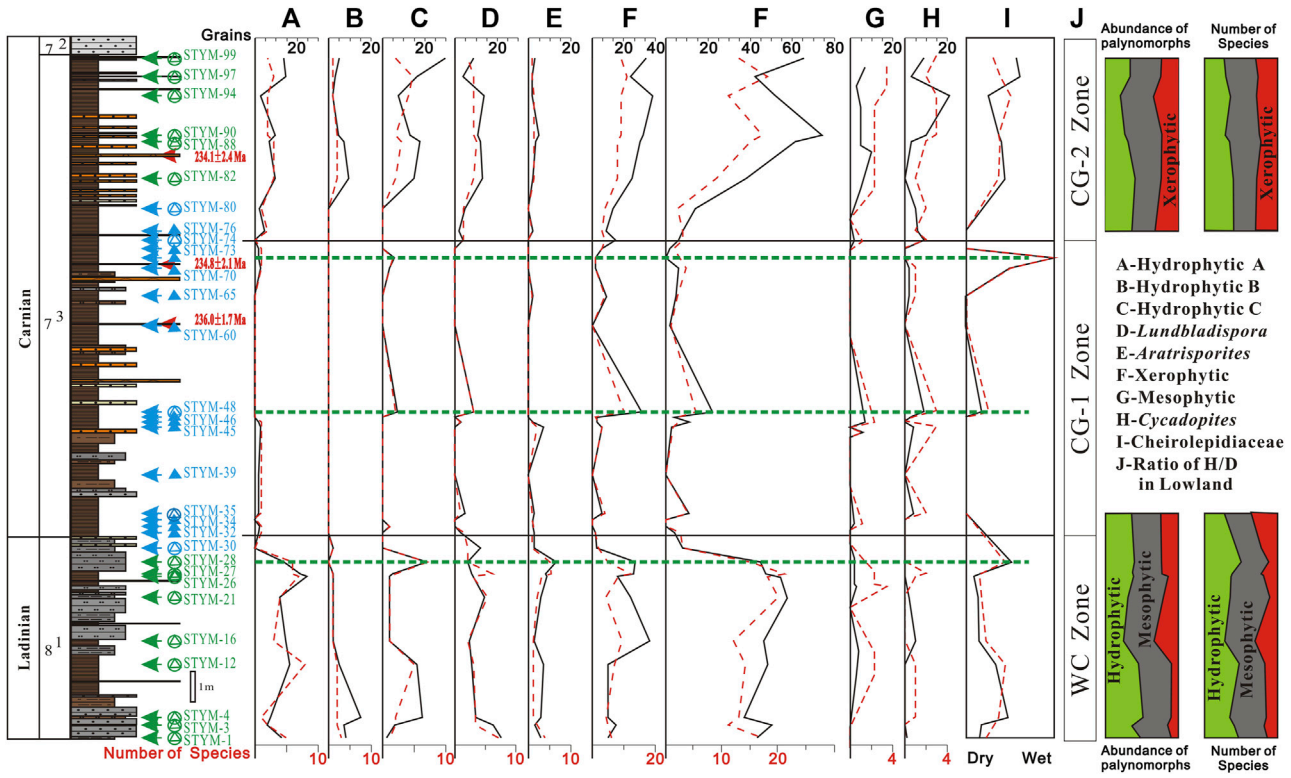

FIGURE 8
Reconstructed humidity based on diversity and abundance of palynofloras at Yunmeng profile, Ordos Basin, China.

were characterized by a decrease in pollen grains normally attributed to xerophytic upland vegetation and an increase in hygrophytic associations attributable to herbaceous Filicopsida (ferns), Lycopodiales (clubmosses), Equisetopsida (horsetails), and Cycadeoidales (Roghi et al., 2010). However, palynological data from the YC7 and YC8 members in the Xifeng area of Qingyang, Shaanxi Province (Ji and Meng, 2006; Ji and Zhu, 2013) might reveal another scenario: the climate in the early Late Triassic might have been as warm and humid as that in the late Middle Triassic. Recent studies in the Jiyuan Basin, Henan Province, China, showed a depositional thickness from the CPE of approximately 40 m in the ZJ-1 borehole based on four of eleven palynological samples scattered in a 140-m thick core (Lu et al., 2021).

Based on previous research (Balme, 1995; Taylor et al., 2009; Zhang J. G. et al., 2021), the botanical affinities, habits, eco-groups, and environments of the palynological taxa were reconstructed for the palynoflora on the Yunmeng profile in the Ordos Basin (Table 2). To better understand climate change, both the abundance of palynomorphs and the diversity at the species level were statistically analyzed (Figure 8). Not included in the analysis were 16 productive samples (STYM-30, -32, 33, -34, -39, -45, -46, -47, -48, -60, -65, -70, -72, -73, -74, and -80) because they included <10 taxa. The other 16 samples were distributed in two groups: the uppermost part of the YC8-1 sub-member and the upper part of the YC7-3 sub-member and were subjected to quantitative analysis (Visscher and Van der Zwan, 1981). The results show that the climates revealed by the two palynofloras were similar, with both vegetation types including hydro-, meso-, and xerophytic elements (Figure 8). The xerophytic plants comprised 11%–38% of the vegetation at the species level and 14%–35% of the total sporo-pollen specimens. Evergreen shrubs, trees, and deciduous arbors were present in the latest Ladinian and early Carnian palynofloras. The hydrophytic plants, including lycophytes, sphenophytes, and pteridophytes, comprised 25%–50% and 20%–51% of the total species and specimens, respectively. The mesophytic plants included Pteridospermophytes, Ullmanniaceae, Majonicaceae, Araucariaceae, Podocarpaceae, Caytoniales, and *Cycadopites*, and comprised 35%–54% and 32%–49% of the total species and specimens, respectively. Therefore, the phytoclimatic compositions of the two palynofloras were generally quite stable. This was also evidenced by the coexistence of gnetalean liana plants (*Chasmatosporites*) in the two palynofloras (Supplementary Appendix S1; Table 2).

However, the compositions of the flora in the two assemblages differed greatly; the WC assemblage in the YC8-1 sub-member included 121 species in 47 genera, while the CG assemblage in the YC7-3 sub-member included only 76 species in 45 genera. The diversity lost at the species level was 38%. Furthermore, examination of the spores showed that 38 species—70% of the spores in the WC assemblage—were lost, including many species from *Aratrisporites*, *Lundbladispora*, *Calamospora*, *Verrucosisporites*, *Cyclogranisporites*, *Asseretospora*, and *Apiculatisporites*. Although the deepening and enlargement of the Triassic Ordos Lake might have led to the mother plants being far from the deep and semi-deep lake deposits, the aquatic *Aratrisporites* also greatly declined, with only one species remaining from the former eight. This might imply that the lake was eutrophic, as also evidenced by the burst of algae and organic-rich oil shales in the YC7-3 sub-member (Liu et al., 2022). Regarding eco-groups (Figure 8), the hydrophytic A and B types are composed of horsetails and herbaceous ferns; they were quite abundant and diverse in the WC zone but rare or absent in the CG zone, especially in the CG-1 sub-zone. Dendroid ferns

also exhibited a similar pattern. Therefore, the lake was eutrophic, and the climate was warm but likely much more arid than before.

Approximately a third of the pollen (26 species of gymnosperm pollen) in the WC assemblage was lost in the CG assemblage. The lost gymnosperms mainly included Peltaspermales, Corystospermales, Voltziales, Araucariaceae, and some old conifers living upland and in dry lowlands as evergreen shrubs and deciduous and evergreen trees, which included the mesophytic and xerophytic plants. Therefore, this decline is less affected by eco-groups, habitats, and climate type, which must be an overall loss. Meanwhile, Cheirolepidiaceae and *Pinuspollenites* emerged, and Utrechtiaceae conical leaf shrubs survived. This also indicates a drier climate. In summary, the loss of spores and pollen in every niche and the emergence of most xerophytic Cheirolepidiaceae plants indicate that the climate became drier when the lake became deeper, broader, and euphytic. This coincided with a strong seasonal monsoon climate under greenhouse conditions.

5.3.3 Monsoon arid climate

The monsoon arid climate might have begun in the latest Ladinian when the flora began to fade at the top of the YC8-1 sub-member (Figure 8). Most hydrophytic and mesophytic plants recovered until the upper part of the YC7-3 sub-member, and even xerophytic plants recovered by adding more xerophytic plants. However, hydrophytic C (dendroid ferns), *Lundbladispora*, *Cycadopites*, and Cheirolepidiaceae exhibited one or two peaks in abundance and diversity in the CG-1 sub-zone. These eco-group peaks in the CG-1 sub-zone appear contradictory; based on these peaks, hydrophytic C, hydrophytic D, and *Cycadopites* favor humid climate, while others such as xerophytic and mesophytic plants, and Cheirolepidiaceae prefer arid environments. *Cycadopites* acme is an indicator of the CPE, together with *Aulisporites astigmousus* acme, in the northern calcareous Alps (Mueller et al., 2016). However, there are no acmes of *Cycadopites* or *A. astigmousus* in the boreal region—for example, Central Spitsbergen (Mueller et al., 2015). Therefore, it is difficult to provide a key palynological indicator for the CPE. Meanwhile, the carbon isotopic stratigraphy of the Ladinian and Carnian deposits in the western and eastern Tethys shows at least four negative excursion episodes (Dal Corso et al., 2012; Dal Corso et al., 2015; Dal Corso et al., 2018; Mueller et al., 2016; Sun et al., 2016; Miller et al., 2017). Recent carbon isotopic chemostratigraphy in the Ordos Basin, together with cyclostratigraphy and isotopic dating, has revealed several negative excursions in the YC8 and YC7 members; however, whether these results are related to Ladinian or Carnian events remains controversial (Zhang K. et al., 2021; Jin et al., 2021).

The latest palynological research in the Carnian amber-bearing section of the Dolomite Alps in Italy sheds light on the primary criteria for identifying the CPE. The coexistence of Majonicaceae (*Lueckisporites*), Voltziaceae (*Triadispora*), Araucariaceae (*Araucariacites*), and Pinaceae (*Abietineaepollenites*) pollen may provide a mark of the CPE (Roghi et al., 2022). In this study, *Lueckisporites* in the Yunmeng profile were only found in sample STYM-04 and *Araucariacites* only in sample STYM-12; moreover, they did not coexist. This might indicate that sample STYM-04 was not the last observation of *Lueckisporites*. Meanwhile, the possibility of pioneering *Araucariacites* cannot be avoided (Tokunaga et al., 1977). If we consider *Abietineaepollenites* for calibration, the lowest record of the genus was in the Erqiao Formation in Guizhou Province, China, which is younger than the Carnian *Neogondolella polygnathiformis* zone (Yang et al., 1995; Shang, 2011); however, the *Araucariacites* were neither recorded there nor in the younger Late Triassic horizons. As the uppermost Falang Formation is aged early Carnian due to the *N. polygnathiformis* zone (Yang et al., 1995), the overlying Erqiao and Banan formations are most probably late Julian–Tuvalian in age (Tong et al., 2019). Therefore, the coexistence of *Dictyophyllidites*, *Lueckisporites*, and *Abietineaepollenites* might be regarded as an indicator of the CPE. Furthermore, *Classopollis* in the Erqiao Formation may be another reference for the event. Therefore, it is reasonable to regard the existence of *Classopollis* and *Dictyophyllidites* as indications of the CPE. Thus, the CPE on the Yunmeng profile in the Ordos Basin can be roughly located in the CG-1 sub-zone (Figure 8). The humid pulse can be recognized by the humidity index of the lowland plants, which is directly related to the fine organic-rich deposit of deep and semi-deep lacustrine environments. At least three humid pulses can be observed on the Yunmeng profile, including two in the early Carnian CG-1 sub-zone (marked by green dashed lines in Figure 8).

6 Conclusion

Detailed palynological investigation of the Yunmeng profile in the Ordos Basin, China, was performed to determine the age and reconstruct its vegetation and climate. The result revealed: 1) two palynological assemblages for the YC8-1 and YC7-3 sub-members, *L. watangensis–T. combinatus* and *L. communis–D. granulus*, respectively; 2) correlation of the GSSP of the Carnian and the Late Triassic floras in South China with marine conodont fossils allowing the assignment of the two assemblages to the latest Ladinian and early Carnian ages, respectively; 3) the coexistence of *Cyathidites minor* (Couper, 1953), *Dictyophyllidites harrisii* (Couper, 1958), *Apiculatisporis bulliensis* (Helby ex De Jersey 1971), *Aratrisporites xiangxiensis* (Li and Shang, 1980), *Piceaepollenites omoriciformis* (Bolkh.) (Xu and Zhang, 1980), *Podocarpidites ornatus* (Pocock, 1962), *Discisporites granulus* (Zhang, 1984), and *Classopollis* (Pflug, 1953) is proposed as an indicator of the Carnian age in the North China palynofloral realm; 4) vegetation changes are obvious, especially in the boundary between the Ladinian and Carnian, in which 70% of ferns and >30% of gymnosperm species were lost; the vegetation changes suggest a strong seasonal arid climate, as indicated by the emergence of Cheirolepidiaceae and *Pinuspollenites*; 5) the climate during latest Ladinian and early Carnian was "hot house," with evergreen shrubs, bushes, and arbor trees flourishing in the tropical Ordos Basin, which was isolated by the Qinling–Dabie orogenic belt mountains from the Tethys to the south; 6) the warm seasonal arid climate might have been interrupted by a monsoonal pluvial pulse, and three strong pulses are signaled in the latest Ladinian and early Carnian based on the humidity index of lowland plants.

Data availability statement

The original contributions presented in the study are included in the article/Supplementary Material; further inquiries can be directed to the corresponding author.

Author contributions

YS and XL proposed the study, collected the samples, identified most part of the palynomorphs, and wrote the original draft; YZ edited

the figures; XS proofread the manuscript; SZ identified some of the sporopollen. All authors have read and agreed to the final version of the manuscript.

Funding

This work is financially supported by the National Natural Science Foundation of China (Grant nos. 41972012 and 31700183) and the State Key Laboratory of Shale Oil and Gas Enrichment Mechanisms and Effective Development (No. GSYKY-B09-33).

Acknowledgments

The authors express their sincere thanks to Prof. Jinnan Tong (China University of Geosciences, Wuhan) for providing constructive discussion on the Triassic deposits in China and to Prof. Quanyou Liu (Institute of Energy, Peking University), Peng Li and Rui Zhang (Petroleum Exploration and Production Research Institute, SINOPEC), and Mingda Zhang (Jilin University, Changchun) for observing organic cumulations and collecting samples in the field. They also thank the two reviewers for their careful and thorough review of the manuscript; their constructive suggestions have considerably strengthened the main topic of the manuscript. Finally, they express their special thanks to Prof. Xing Xu (Associate Editor-in-Chief) for graciously handling this report.

Conflict of interest

The authors declare that the research was conducted in the absence of any commercial or financial relationships that could be construed as a potential conflict of interest.

Publisher's note

Supplementary material

The Supplementary Material for this article can be found online at: https://www.frontiersin.org/articles/10.3389/feart.2022.1008707/full#supplementary-material

SUPPLEMENTARY APPENDIX S1
Stratigraphy of the Yunmeng profile showing isotopic dating and productive palynological samples. Results of the quantitative sporo-pollen analysis (number).

SUPPLEMENTARY APPENDIX S2
Description of the species in the Yunmeng Profile.

References

Arjang, B. (1975). The Rhaetian-Jurassic flora of Iran and Afghanistan. 1. The microflora of the Rhaetian-Jurassic deposits of the kerman basin (central Iran). *Palaeontogr. Abt. B* 152 (4), 85–148.

Balme, B. E. (1995). Fossil *in situ* spores and pollen grains: An annotated catalogue. *Rev. Palaeobot. Palynology* 87, 81–323. doi:10.1016/0034-6667(95)93235-X

Balme, B. E. (1963). Plant microfossils from the Lower Triassic of western Australia. *Palaeontology* 6 (1), 12–40.

Benton, M. J., and Newell, A. J. (2014). Impacts of global warming on Permo-Triassic terrestrial ecosystems. *Gondwana Res.* 25, 1308–1337. doi:10.1016/j.gr.2012.12.010

Bharadwaj, D. C., and Singh, H. P. (1964). An Upper Triassic miospore assemblage from the coals of Lunz, Austria. *Palaeobotanist* 12 (1), 28–44. doi:10.54991/jop.1963.641

Bolkhovitina, N. A. (1956). *Atlas of spores and pollen from Jurassic and Lower Cretaceous deposits of the vilyui depression*. USSR Transactions of the Institute of Geology Academy of Sciences, 1–188. (in Russian).

Boucot, A. J., Chen, X., Scotese, C. R., and Fan, X. X. (2009). *Phanerozoic paleoclimate reconstruction of the world*. Beijing: Science Press.

Brandner, R. (1984). Meeresspiegelschwankungen und Tektonik in der Trias der NW–Tethys. *Jahrb. Geol. Bundesanst.* 126 (4), 435–475.

Bureau of Geology and Mineral Resources of Shaanxi Province (1998). *Stratigraphy (lithostratic) of Shaanxi Province*. Wuhan: China University of Geosciences Press.

Césari, S. N., and Colombi, C. (2016). Palynology of the Late Triassic ischigualasto formation, Argentina: Paleoecological and paleogeographic implications. *Palaeogeogr. Palaeoclimatol. Palaeoecol.* 449, 365–384. doi:10.1016/j.palaeo.2016.02.023

Chitaley, S. D., and McGregor, D. C. (1988). *Bisporangiostrobus harrisii* gen. et sp. nov. an eligulate lycopsid cone with *Duosporites* megaspores and *Geminospora* microspores from the Upper Devonian of Pennsylvania. *U.S.A. Palaeontogr. Abt. B* 210 (4–6), 127–149.

Clarke, R. F. A. (1965). Keuper miospores from worcetershire, England. *Palaeontology* 8 (2), 294–321.

Colombi, C., Martínez, R. N., Césari, S., Alcober, O., and Montanez, I. (2021). A high-precision U-Pb zircon age constraints the timing of the faunistic and palynofloristic events of the Carnian Ischigualasto Formation, San Juan, Argentina. *J. S. Am. Earth Sci.* 111 (6), 103433. doi:10.1016/j.jsames.2021.103433

Cookson, I. C. (1947). *Plant microfossils from the lignites of kerguelen archipelago*. New Zealand Antarctic Res Expedition, 127–142. Reports Series A2.

Couper, R. A. (1958). British Mesozoic microspores and pollen grains. A systematic and stratigraphic study. *Palaeontogr. Abt. B -Stuttgart-* 103 (4–6), 75–179.

Couper, R. A. (1953). Upper Mesozoic and Cainozoic spores and pollen grains from New Zealand. *Paleontol. Bull. N. Z. Geol. Surv.* 22, 1–77.

Cuneo, N. R., Taylor, E. L., Taylor, T. N., and Krings, M. (2003). *In situ* fossil forest from the upper Fremouw Formation (Triassic) of Antarctica: Paleoenvironmental setting and paleoclimate analysis. *Palaeogeogr. Palaeoclimatol. Palaeoecol.* 197, 239–261. doi:10.1016/S0031-0182(03)00468-1

Dal Corso, J., Gianolla, P., Newton, R. J., Franceschi, M., Roghi, G., Caggiati, M., et al. (2015). Carbon isotope records reveal synchronicity between carbon cycle perturbation and the "Carnian Pluvial Event" in the Tethys realm (Late Triassic). *Glob. Planet. Change* 127, 79–90. doi:10.1016/j.gloplacha.2015.01.013

Dal Corso, J., Gianolla, P., Rigo, M., Franceschi, M., Roghi, G., Mietto, P., et al. (2018). Multiple negative carbon-isotope excursions during the carnian pluvial episode (late triassic). *Earth-Science Rev.* 185, 732–750. doi:10.1016/j.earscirev.2018.07.004

Dal Corso, J., Mietto, P., Newton, R. J., Pancost, R. D., Preto, N., Roghi, G., et al. (2012). Discovery of a major negative $\delta^{13}C$ spike in the Carnian (Late Triassic) linked to the eruption of Wrangellia flood basalts. *Geology* 40 (1), 79–82. doi:10.1130/G32473.1

De Jersey, N. J. (1972). Triassic miospores from the esk beds. *Publ. Geol. Surv. Queensl., 357, Palaeontol. Pap.* 32, 1–40.

De Jersey, N. J. (1971). Triassic miospores from the tivoli formation and kholo sub-group. *Publ. Geol. Surv. Queensl.* 353, 1–40.

De Jersey, N. J. (1964). Triassic spores and pollen grams from the Bundamba Group. *Publ. Geol. Surv. Queensl.* 321, 1–21.

De Jersey, N. J. (1962). Triassic spores and pollen grams from the Ipswich Coalfield. *Publ. Geol. Surv. Queensl.* 307, 1–18.

Deng, S. H., Lu, Y. Z., Luo, Z., Fan, R., Li, X., Zhao, Y., et al. (2018). Subdivision and age of the Yanchang Formation and the Middle/Upper Triassic boundary in Ordos Basin, North China. *Sci. China Earth Sci.* 61, 1419–1439. doi:10.1007/s11430-017-9215-3

Domeier, M., and Torsvic, T. H. (2014). Plate tectonics in the Late Paleozoic. *Geosci. Front.* 5, 303–350. doi:10.1016/j.gsf.2014.01.002

Donofrio, D. A. (1991). "Radiolaria and porifera spiculae from the Upper Triassic of aghdarband (ne–Iran)," in *The Triassic of aghdarband, AqDarband ne–Iran, and its pre-Triassic frame*. Editor A. W. Ruttner (Abhandlungen der Geologischen Bundesanstalt), 38, 205–223.

Du, B. A. (1985). Middle triassic palynological assemblage in the Wangjiashn basin of Jingyuan, Gansu and its stratigraphical significance. *Acta Bot. Sin.* 27 (5), 538–544. (in Chinese with English abstract).

Dubiel, R. F., Parrish, J. T., Parrish, J. M., and Good, S. C. (1991). The pangaean megamonsoon: Evidence from the Upper Triassic chinle formation, Colorado plateau. *Soc. Sediment. Geol.* 6 (4), 347–370. doi:10.2307/3514963

ECSDC (Editorial Committee of Stratigraphic Dictionary of China) (2000). *Stratigraphic dictionary of China:Triassic system*. Beijing: Geological Publishing House.

Fedo, C. M., Sircombe, K. N., and Rainbird, R. H. (2003). Detrital zircon analysis of the sedimentary record. *Rev. Mineralogy Geochem.* 53, 277–303. doi:10.2113/0530277

Fisher, M. J., and Bujak, J. (1975). Upper Triassic palynofloras from arctic Canada. *Proc. Annu. Meet. Am. Assoc. Stratigr. Palynologists* 11 (6), 87–94. doi:10.2307/3687224

Gair, H. S., Norris, G., and Ricker, J. (1965). Early Mesozoic microfloras from Antarctica. *N. Z. J. Geol. Geophys.* 8 (2), 231–235. doi:10.1080/00288306.1965.10428109

Geiger, M. E., and Hopping, C. A. (1968). Triassic stratigraphy of the southern North sea basin. *Philosophical Trans. R. Soc. B Biol. Sci.* 254 (790), 1–36. doi:10.1098/rstb.1968.0012

Gradstein, F. M. (1971). The age of Beds in the Lettenkohle facies in South-East France (A palynological approach). *Pollen Spores* 13 (1), 169–178.

Grauvogel-Stamm, L., and Lugardon, B. (2004). The spores of the Triassic lycopsid *Pleuromeia sternbergii* (münster) corda: Morphology, ultrastructure, phylogenetic implications, and chronostratigraphic inferences. *Int. J. Plant Sci.* 165 (4), 631–650. doi:10.1086/386562

Halle, T. G. (1908). Bidrag till kannedomen om skandinaviens Amphipoda gammaridea. *K. Sven. vetenskapsakademiens Handl.* 43i (1), 1–104. doi:10.5962/bhl.part.28297

Harland, W. B. (1997). *The geology of Svalbard*. London: Geological Society Press.

Harris, T. M. (1937). The fossil flora of scoresby sound east Greenland: Part 5. Stratigraphic relations of the plant beds. *Meddelel Ser. Om. Grønl.* 112, 82–86.

Hart, G. F. (1964). A review of the classification and distribution of the Permian miospore: Disacciti Striatiti. *Congrès Int. de Stratigr. de géologie du Carbonifère* 5, 1171–1199.

Hornung, T., and Brandner, R. (2005). Biochronostratigraphy of the Reingraben turnover (Hallstatt facies belt), local black shale events controlled by regional tectonics, climatic change and plate tectonics. *Facies* 51, 460–479. doi:10.1007/s10347-005-0061-x

Horowitz, A. (1973). Triassic miospores from southern Israel. *Rev. Palaeobot. Palynology* 16 (3), 175–207. doi:10.1016/0034-6667(73)90045-6

IGCAGS (Institute of Geology, Chinese Academy of Geological Sciences) (1980). *Mesozoic stratigraphy and palaeontology of Ordos Basin*. Beijing: Geological Publishing House Press.

Jansonius, J. (1962). Palynology of Permian and Triassic sediments, peace river area, western Canada. *Palaeontogr. Abt. B Band.* 110, 35–98.

Ji, L. M., and Meng, F. W. (2006). Palynology of Yanchang Formation of Middle and Late Triassic in eastern Gansu Province and its paleoclimatic significance. *J. China Univ. Geosciences* 17 (3), 209–220. doi:10.1016/S1002-0705(06)60030-7

Ji, L. M., and Zhu, Y. H. (2013). Sporo-pollen assemblages and paleoclimate of the Yanchang Formation in the Xifeng area, southwestern Ordos Basin, Gansu Province, NW China. *Acta Micropalaeontologica Sin.* 30 (4), 367–378.

Ji, L. X., Liu, F., Luo, W., and Ouyang, S. (2017). Spores-pollen from Early Triassic deposits in Qinghai Province and their stratigraphic significance. *J. Stratigr.* 41 (4), 450–466. (in Chinese with English abstract). doi:10.19839/j.cnki.dcxzz.2017.04.012

Ji, L. X., Liu, F., Luo, W., and Ouyang, S. (2015). Triassic sporopollen and acritarchs from northern Qilian Mountain (Qinghai) and their stratigraphical significance. *J. Stratigr.* 39 (4), 367–379. (in Chinese with English abstract). doi:10.19839/j.cnki.dcxzz.2015.04.003

Jin, X., Baranyi, V., Caggiati, M., Franceschi, M., Wall, C. J., Liu, G. L., et al. (2021). Middle Triassic lake deepening in the Ordos Basin of North China linked with global sea-level rise. *Glob. Planet. Change* 207 (2), 103670. doi:10.1016/j.gloplacha.2021.103670

Jin, X., McRoberts, C. A., Shi, Z. Q., Mietto, P., Rigo, M., Roghi, G., et al. (2019). The aftermath of the CPE and the Carnian–Norian transition in northwestern sichuan basin, south China. *J. Geol. Soc.* 176 (1), 179–196. doi:10.1144/jgs2018-104

Kent, D. V., and Olsen, P. E. (2000). Magnetic polarity stratigraphy and paleolatitude of the Triassic–Jurassic blomidon Formation in the fundy basin (Canada): Implications for early Mesozoic tropical climate gradients. *Earth Planet. Sci. Lett.* 179 (2), 311–324. doi:10.1016/S0012-821X(00)00117-5

Kimyai, A. (1977). *Further information on the palynological stratigraphy of the Mesozoic Coaly sediments from Kerman*. IranTehran: Iranian Petroleum Institute, Proceeding of the 2nd Geological Symposium of Iran, 191–217. (in Persian).

Klaus, W. V. (1960). Sporen der karnischen stufe der ostalpinen Trias. *Jahrb. Geol. Bundesanst.* 5, 107–183.

Krassilov, V. A., Afonin, S. A., and Naugolnykh, S. V. (1999). *Permotheca* with *in situ* pollen grains from the Lower Permian of the urals. *Palaeobotanist* 49 (1), 19–25. doi:10.54991/jop.1999.1287

Krutzsch, W. (1955). Uber einige liassishe "angiospermide" sporomorphen. *Z Geol.* 4, 65–76.

Kustatscher, E., and Van Konijnenburg-van Cittert, J. H. A. (2010). Seed ferns and cycadophytes from the Triassic flora of thale (Germany). *Neues Jahrb. für Geol. Paläontologie - Abh.* 258 (2), 195–217. doi:10.1127/0077-7749/2010/0097

Kutzbach, J. E., and Gallimore, R. G. (1989). Pangaean climates: Megamonsoons of the megacontinent. *J. Geophys. Res.* 93 (3), 3341–3357. doi:10.1029/JD094iD03p03341

Lele, K. M. (1964). Studies in the talchir flora of India: 2. Resolution of the spore genus nuskoisporites pot. & KL. *Palaeobot.* 12 (2), 147–168. doi:10.54991/jop.1963.651

Leschik, G. (1955). Die Keuperflora yon Neuwelt bei Basel. II. Die Iso-und Mikrosporen. *Schweiz. Paläontologische Abh.* 71, 1–70.

Li, L. Q., Wang, Y. D., Kürschner, W. M., Ruhl, M., and Vajda, Vivi. (2020). Palaeovegetation and palaeoclimate changes across the Triassic–Jurassic transition in the Sichuan Basin, China. *Palaeogeogr. Palaeoclimatol. Palaeoecol.* 556 (15), 109891. doi:10.1016/j.palaeo.2020.109891

Li, W. B., and Shang, Y. K. (1980). Sporo-pollen assemblages from the Mesozoic coal series of Western hubei. *Acta Palaeontol. Sin.* 19 (3), 201–219. (in Chinese with English abstract). doi:10.19800/j.cnki.aps.1980.03.004

Li, Y., Yao, J. X., Wang, S. E., and Pang, Q. Q. (2016). Middle-Late Triassic terrestrial strata and establishment of stages in the Ordos Basin. *Acta Geosci. Sin.* 37 (3), 267–276. doi:10.3975/cagsb.2016.03.02

Liu, Q. Y., Li, P., Jin, Z. J., Sun, Y. W., Hu, G., Zhu, D. Y., et al. (2022). Organic-rich formation and hydrocarbon enrichment of lacustrine shale strata: A case study of chang 7 member. *Sci. China Earth Sci.* 65, 118–138. doi:10.1007/s11430-021-9819-y

Liu, Z. S., Li, L. Q., and Wang, Y. D. (2015). Late triassic spore-pollen assemblage from the Xujiahe Formation in hechuan of chongqing, China. *Acta Palaeontol. Sin.* 54 (3), 279–304. (in Chinese with English abstract). doi:10.19800/j.cnki.aps.2015.03.001

Liu, Z. S., Shang, Y. K., and Li, W. B. (1981). Triassic and Jurassic spore-pollen assemblages from some localities of Shaanxi and Gansu, north-west China. *Bull. Nanjing Inst. Geol. Palaeontol. Chin. Acad. Sci.* 3, 131–210. (in Chinese).

Lu, J., Zhang, P. X., Dal Corso, J., Yang, M. F., Wignall, P. B., Greene, S. E., et al. (2021). Volcanically driven lacustrine ecosystem changes during the carnian pluvial episode (Late Triassic). *Proc. Natl. Acad. Sci. U. S. A.* 118 (40), e2109895118. doi:10.1073/pnas.2109895118

Ma, X. H., Xing, L. S., Yang, Z. Y., Xu, S. J., and Zhang, J. X. (1993). Paleomagnetic study since late Paleozoic in the Ordos Basin. *Acta Geophys. Sin.* 36 (1), 68–79. (in Chinese with English abstract).

Mädler, K. (1964). Die geologische Verbreitungvon Sporen und Pollen in der deutschen Trias. *Beih. Zum Geol. Jahrb.* 65, 1–145.

Malyavkina, V. S. (1949). Determination key of spores and pollen, Jurassic-Cretaceous. *Tr. Vsesoyuznogo Neft. Naucho-Issledovatel Skogo Geologo-Razvedochnogo Instituta* 33, 1–137.

Mamay, S. H. (1950). Some American Carboniferous fern fructifications. *Ann. Mo. Botanical Gard.* 37 (3), 409–476. doi:10.2307/2394515

Mander, L., Kurschner, W. M., and Mcelwain, J. C. (2010). An explanation for conflicting records of Triassic-Jurassic plant diversity. *Proc. Natl. Acad. Sci.* 107 (35), 15351–15356. doi:10.1073/pnas.1004207107

Miao, S. J., Yu, J. X., Qu, L. F., Zhang, W. P., Zhang, Q. H., and Zhang, D. H., (1984). Mesozoic spores and pollen. In *Tianjin Institute of Geology and mineral Resources*. Palaeontological Atlas of North China, 3. Micropaleontoloy Geological Publishing House Press, 440–638 (in Chinese with English abstract).

Mietto, P., Manfrin, S., Preto, N., Rigo, M., Roghi, G., Furin, S., et al. (2012). The global boundary stratotype section and point (GSSP) of the carnian stage (Late Triassic) at prati di Stuores/stuores wiesen section (southern Alps, NE Italy). *Episodes* 35 (3), 414–430. doi:10.18814/epiiugs/2012/v35i3/003

Miller, C. S., Peterse, F., da Silva, A. C., Baranyi, V., Reichart, G. J., and Kürschner, W. M. (2017). Astronomical age constraints and extinction mechanisms of the late Triassic Carnian crisis. *Sci. Rep.* 7 (1), 2557. doi:10.1038/s41598-017-02817-7

Mueller, S., Hounslow, M. W., and Kurschner, W. M. (2015). Integrated stratigraphy and palaeoclimate history of the carnian pluvial event in the boreal realm: New data from the Upper Triassic kapp toscana group in central spitsbergen (Norway). *J. Geol. Soc.* 173 (1), 186–202. doi:10.1144/jgs2015-028

Mueller, S., Krystyn, L., and Kurschner, W. M. (2016). Climate variability during the carnian pluvial phase - a quantitative palynological study of the Carnian sedimentary succession at lunz am see, northern calcareous Alps, Austria. *Palaeogeogr. Palaeoclimatol. Palaeoecol.* 441, 198–211. doi:10.1016/j.palaeo.2015.06.008

Mutti, M., and Weissert, H. (1995). Triassic monsoonal climate and its signature in Ladinian-Carnian carbonate platforms (Southern Alps, Italy). *J. Sediment. Res.* 65 (3), 357–367.

Nilsson, T. (1958). *Uber das Vorkommen eines mesozoischen Sapropelgesteins in Schonen*. Sweden: Lunds Universitets Arsskrift Press.

Ouyang, S., Ji, L. X., and Luo, W. (2011). Early Triassic spore-pollen assemblages from the Hongshuichuan Group of central-Western Qinghai. *Acta Palaeontol. Sin.* 50 (2), 187–218. (in Chinese with English abstract). doi:10.19800/j.cnki.aps.2011.02.005

Ouyang, S., and Li, Z. P. (1980). "Microflora from the Kayitou Formation of Fuyuan district, E. Yunnan and its bearing on stratigraphy and palaeobotany," in *Nanjing Institute of Geology and palaeontology, academia sinica* (Beijing: Stratigraphy and Palaeontologyof Upper Permian Coal-Bearing Formation in Western Guizhou and Eastern YunnanScience Press), 123–194. (in Chinese).

Ouyang, S. (1982). Upper Permian and Lower triassic palynomorphs from eastern yunnan, China. *Can. J. Earth Sci.* 19 (1), 68–80. doi:10.1139/e82-006

Pan, Z. X. (1934). *Oil shale geology in northern Shaanxi*. Central Geological Survey, Geological Report.

Pang, J. G., Li, W. H., and Chen, Q. H. (2010). Characteristics and deposition of marker beds in the Yanchang Formation of the northern Shaanxi. *J. Stratigr.* 34 (2), 173–178. (in Chinese with English abstract). doi:10.19839/j.cnki.dcxzz.2010.02.011

Parrish, J. T. (1993). Climate of the supercontinent Pangea. *J. Geol.* 101 (2), 215–233. doi:10.1086/648217

Paterson, N. W., Mangerud, G., and Mørk, A. (2016). Late triassic (early carnian) palynology of shallow stratigraphical core 7830/5-U-1, offshore kong karls land, Norwegian arctic. *Palynology* 41 (1), 230–254. doi:10.1080/01916122.2016.1163295

PCOC (PetroChina Changqing Oilfield Company) (1992). *Petroleum geology of China*, Vol. 12. Beijing: Petroleum Industry Press. (in Chinese).

Pflug, H. D. (1953). Origin and development of the angiosperm pollen in Earth history. *Palaeontogr. Abt. B* 95, 61–171.

Planderova, E. (1972). A contribution to palynological research of lunz beds in west carpathian region. *Geol. Pr. Spravy* 58, 57–77.

Playford, G., and Dettmann, M. E. (1965). Rhaeto-liassic microfossils from the leigh creek coal measures, south Australia. *Senckenberg; Lethaea* 46 (2/3), 127–181.

Playford, G. (1965). Plant microfossils from triassic sediments near poatina, tasmania. *J. Geol. Soc. Aust.* 12 (2), 173–210. doi:10.1080/00167616508728592

Pocock, S. A. J. (1962). Microfloral analysis and age determination of strata at the Jurassic-Cretaceous boundary in the Western Canada Plains. *Palaeontogr. Abt. B* 111 (1–3), 1–95.

Pocock, S. A. J. (1970). Palynology of the jurassic sediments of Western Canada. Part I and II. *Palaeontogr. Abt. B* 130, 12–136.

Potonié, R., and Klaus, W. (1954). Einige Sporengattungen des alpinen Sazgebirges. *Geol. Jahrb.* 68, 517–544.

Preto, N., and Hinnov, L. A. (2003). Unraveling the origin of carbonate platform cyclothems in the Upper Triassic durrenstein formation (dolomites, Italy). *J. Sediment. Res.* 73 (5), 774–789. doi:10.1306/030503730774

Preto, N., Kustatscher, E., and Wignall, P. B. (2010). Triassic climates-state of the art and perspectives. *Palaeogeogr. Palaeoclimatol. Palaeoecol.* 290 (1–4), 1–10. doi:10.1016/j.palaeo.2010.03.015

Qu, L. F. (1984). "Palaeontological atlas of North China, 3. Micropaleontology," in *Tianjin Institute of Geology and mineral Resources* ((Beijing: Ceological Publishing House Press), 538–573. (in Chinese with English abstract).

Qu, L. F. (1982). The palynological assemblage from the Liujiagou formation of Jiaocheng, Shanxi. *Bull. Geol. Inst. Chin. Acad. Geol. Soc.* 4, 83–93. (in Chinese with English abstract).

Qu, L. F. (1980). "Triassic spores and pollen," in *Mesozoic stratigraphy and palaeontology of the shanxi-cansu-ningxia basin (1)Institute of ceology, Chinese academy of geological sciences* (Beijing: Geological Publishing House Press), 115–143. (in Chinese).

Qu, L. F., and Wang, Z. (1990). "Triassic palynological assemblages in North xinjiang," in *Permian to tertiary strata and palynological assemblages in the North of xinjiang* (Xinjiang Petroleum Administration (Beijing: Institute of Geology, Chinese Academy of Geological Sciences, Research Institute of Petroleum Exploration and DevelopmentChina Environment Science Press), 37–56. (in Chinese with English abstract).

Qu, L. F., and Wang, Z. (1986). "Triassic sporopollen," in *Permian and Triassic strata and fossil assemblages in the Dalongkou area of Jimsar* (Xinjiang, (Beijing: Institute of Geology, Chinese Academy of Geological Sciences & Institute of Geology, Xinjiang Bureau of Geology and Mineral Resources, Geological Publishing House Press), 111–173.

Retallack, G. J. (1997). Earliest Triassic origin of Isoetes and quillwort evolutionary radiation. *J. Paleontology* 71, 500–521. doi:10.1017/S0022336000039524

Rigo, M., Preto, N., Roghi, G., Tateo, F., and Mietto, P. (2007). A rise in the carbonate compensation depth of Western Tethys in the Carnian (Late Triassic): Deep-water evidence for the carnian pluvial event. *Palaeogeogr. Palaeoclimatol. Palaeoecol.* 246 (2–4), 188–205. doi:10.1016/j.palaeo.2006.09.013

Roghi, G., Gianolla, P., Kustatscher, E., Schmidt, A. R., and Seyfullah, L. (2022). An exceptionally preserved terrestrial record of LIP effects on plants in the Carnian (Upper Triassic) amber-bearing section of the dolomites, Italy. *Front. Earth Sci.* 10, 900586. doi:10.3389/feart.2022.900586

Roghi, G., Gianolla, P., Minarelli, L., Pilati, C., and Preto, N. (2010). Palynological correlation of carnian humid pulses throughout western Tethys. *Palaeogeogr. Palaeoclimatol. Palaeoecol.* 290, 89–106. doi:10.1016/j.palaeo.2009.11.006

Rouse, C. E. (1959). Plant microfossils from kootenay coal-measures strata of British columbia. *Micropalaeontology* 5 (3), 303–324. doi:10.2307/1484422

Ruttner, A. W., Brandner, B., and Kirchner, E. (1991). "Geology of the aghdarband area (kopet dagh, ne–Iran)," in *The triassic of aghdarband (AqDarband), ne–Iran, and its pre–triassic frame*. Editor A. W. Ruttner (Abhandlungen der Geologischen Bundesanstalt), 38, 7–81.

Sakulina, G. V. (1973). "Middle and Late Triassic miospores from southeastern Kazakhstan," in *Mikrofossilii drevneishikh otlozhenii. Proceedings of the 3rd international palynological conference*. Editors T. F. Vozzhennikova and T. B. Timofeev (Moscow: Nauka), 33–38.

Scheuring, B. W. (1970). Palynologische und palynostratigraphische untersuchungen des Keupers im bolchentunnel (Solothurner Jura). *Schweiz. Palaontologische Abh.* 88, 1–119.

Scheuring, B. W. (1966). Preliminary report on pollen analitical investigations of the upper meridekalke on mount san giorgio (sudtessin). *Eclogae Geol. Helvetiae* 59 (2), 964–965.

Schlager, W., and Schollnberger, W. (1974). Das prinzip stratigraphischer wenden in der Schichtfolge der Nordlichen kalkalpen. *Mitteilungen der Geol. Gesellschaft Wien* 66/67, 165–193.

Schulz, E. (1964). Spores and pollen of the middle buntsandstein of the German basin. *Monatsberichte Dtsch. Akad. Wisssenschaften, Berl.* 6 (8), 597–606.

Schulz, E. (1967). Study of fossil spores from Rhaetian-Liassic Layers in the central part of the German Basin. *Palaeontogr. Abt. B. Palaobotanik* 2 (3), 543–644.

Schuurman, W. M. (1977). Aspects of Late Triassic palynology. 2. Palynology of the "Gres et Schiste a Avicula contorta" and "Argiles de Levallois" (Rhaetian) of northeastern France and southern Luxemburg. *Rev. Palaeobot. Palynology* 23 (3), 159–253. doi:10.1016/0034-6667(77)90007-0

Sedova, M. A. (1956). The definition of four genera of disaccate Striatiti. *Material Palaeontol.* 12, 246–249.

Semenova, E. V. (1987). Miospores from the Triassic deposits in the South-Western regions of the Ukraine. (The fore-dobrogean trough). *Geol. Zhurnal* 47 (5), 66–70.

Seyfullah, L., Kustatscher, E., and Taylor, W. A. (2013). The first discovery of *in situ Verrucosisporites applanatus* spores from the Middle Triassic flora from Bromsgrove (Worcestershire, UK). *Rev. Palaeobot. Palynology* 197, 15–25. doi:10.1016/j.revpalbo.2013.04.004

Shang, Y. K. (2011). *Late Triassic palynology of Yunnan and Guizhou*. China. Beijing: Geological Publishing House Press. (in Chinese).

Shi, X., Lang, J. B., Shu, W. C., Li, H., and Yu, J. X. (2021). Fossil woods from the olenekian (late Early Triassic) Shaofanggou Formation in the Junggar basin, northern Xinjiang, north-west China. *Geol. J.* 56 (12), 6223–6230. doi:10.1002/gj.4193

Shi, Z. Q., Ou, L. H., Luo, F. Z., Li, Y., and Qian, L. J. (2009). Black shale event during the Late Triassic Carnian age: Implications from sedimentary and palaeontological records in Longmen Mountains region. *J. Palaeogeogr.* 11 (4), 375–383. (in Chinese with English abstract).

Shugaevskaya, O. V. (1969). Spores *Duplexisporites* in upper Mesozoic deposits of the river gerbikan (uda depression). *Fossil Fauna Flora ofthe Far East*, 1, 153–160.

Simms, M. J., and Ruffell, A. H. (1990). Climatic and biotic change in the Late Triassic. *J. Geol. Soc.* 147 (1), 321–327. doi:10.1144/gsjgs.147.2.0321

Singh, C. (1964). Microflora of the Lower Cretaceous mannville group, east-central alberta. *Res. Counc. Bull. Alta.* 15, 1–239.

Smith, A. H. V., and Butterworth, M. A. (1967). Miospores in coal seams of the carboniferous of great britain. *Special Pap. Palaeontol.* 1, 1–324.

Smith, D. G. (1974). Late Triassic pollen and spores from the kapp toscana formation, hopen, svalbard: A preliminary account. *Rev. Palaeobot. Palynology* 17, 175–178. doi:10.1016/0034-6667(74)90098-0

Song, Z. C., Shang, Y. K., Liu, Z. S., Huang, P., Wang, X. F., Qian, L. J., et al. (2000). "The Mesozoic spores and pollen," in *Fossil spores and pollen of China*. Z. C. Song Y. K. Shang, et al. (Beijing: Science Press), 2. (in Chinese).

Strullu-Derrien, C., McLoughlin, S., Philippe, M., Mork, A., and Strullu, D. G. (2012). Arthropod interactions with bennettitalean roots in a triassic permineralized peat from hopen, svalbard archipelago (arctic). *Palaeogeogr. Palaeoclimatol. Palaeoecol.* 348–349, 45–58. doi:10.1016/j.palaeo.2012.06.006

Sun, G., Meng, F. S., Qian, L. J., and Ouyang, S. (1995). "Triassic floras," in *Floras of geological age in China*. Editor X. X. Li (Guangzhou: Guangdong Science and Technology Publishing House Press), 229–259. (in Chinese with translation into English by the authors).

Sun, Y. D., Wignall, P. B., Joachimski, M. M., Bond, D. P. G., Grasby, S. E., Lai, X. L., et al. (2016). Climate warming, euxinia and carbon isotope perturbations during the Carnian (Triassic) crisis in South China. *Earth Planet. Sci. Lett.* 444, 88–100. doi:10.1016/j.epsl.2016.03.037

Sun, Y. W., Li, X., Liu, Q. Y., Zhang, M. D., Li, P., Zhang, R., et al. (2020). In search of the inland carnian pluvial event: Middle–Upper Triassic transition profile and U-Pb isotopic dating in the Yanchang Formation in Ordos Basin, China. *Geol. J.* 55 (7), 4905–4919. doi:10.1002/gj.3691

Taylor, T. N., Taylor, E. L., and Krings, M. (2009). *Paleobotany: The Biology and evolution of fossil plants*. 2nd ed. San Diego: Academic Press.

Tokunaga, S., Oshima, H., and Ito, Y. (1977). Recent status and problems of pollen stratigraphy. *J. Geogr. (Chigaku Zasshi)* 86 (2), 73–79. doi:10.5026/jgeography.86.2_73

Tong, J. N., Chu, D. L., Liang, L., Shu, W. C., Song, H. J., Song, T., et al. (2019). Triassic integrative stratigraphy and timescale of China. *Sci. China Earth Sci.* 62, 189–222. (in Chinese). doi:10.1007/s11430-018-9278-0

Tuzhikova, V. I. (1975). "New data on spore-pollen complexes of the Ladinian deposts of the urals," in *New miospores, foraminifera, ostracods and conodonts of the paleozoic and mesozoic of the urals. Collected articles on the problems of stratigraphy. Trudy uralskii nauchnyi tsentralnykh, instituta geologii i geokhimii*. Editors N. P. Malachova and B. I. Chuvashev (Akademiya Nauk SSR), 119, 3–13.

Tuzhikova, V. I. (1979). "On the age and extent of the surakaisk suite and bukobaisk series of the southern cis-urals," in *Triassic stratigraphy of the urals and cis-urals. Symposium on the problems of stratigraphy. Trudy uralskii nauchnyi tsentralnykh, instituta geologii i geokhimii*. Editors V. I. Tuzhikova and G. N. Papulov (Sverdlovsk: Akademiya Nauk SSR), 147, 26–51.

Tuzhikova, V. I.(1980). "On the dating of the deposits of the turinsk phytostratigraphy horizon, turinsk and bitkuyevskaya suites of the suhoyaksk region chelyabinsk basin," in *New data on the triassic stratigraphy of the paleo-urals. Akademiya nauk SSSR, uralskii nauchnyi tsentralnykh, trudy instituta geologii i geokhimii*. Editors V. I. Tuzikova and G. N. Papulov

Varyukhina, L. M. (1961). Spores and pollen of triassic deposites of the southern pechora basin. *Dokl. Akad. Nauk. SSSR* 138 (3), 631–634.

Vasilevskaya, N. D. (1972). "The Late Triassic flora of svalbard," in *Mesozoic deposits in svalbard*. Editors V. N. Sokolov and N. D. Vasilevskaya (NIIGA: Leningrad Press), 27–63.

Vinogradova, K. V. (1974). Miospore assemblages of Triassic sediments of southern mangyshlak. *Dokl. Akad. Nauk. SSSR* 215 (1), 15–18.

Visscher, H., and Brugman, W. A. (1981). Ranges of selected palynomorphs in the alpine Triassic of Europe. *Rev. Palaeobot. Palynology* 34 (1), 115–128. doi:10.1016/0034-6667(81)90069-5

Visscher, H., and van der Zwan, C. J. (1981). Palynology of the circum-mediterranean triassic: Phytogeographical and palaeoclimatological implications. *Geol. Rundsch.* 70, 625–634. doi:10.1007/BF01822140

Wang, Y. D., Jiang, D. X., and Xie, X. P. (2003). Late Triassic palynoflora and its environmental significance of Tuweihe Shaanxi. *Acta Sedimentalogica Sin.* 21 (3), 434–440. (in Chinese with English abstract). doi:10.14027/j.cnki.cjxb.2003.03.011

Wang, Y. Y., Zhang, B., Shi, Z. Q., and Yi, H. S. (2012). Oxygen and carbon isotopic records of the Late Triassic Carnian pluvial event deposits in northwestern Sichuan Province. *J. Palaeogeogr.* 14 (3), 375–382. (in Chinese with English abstract). doi:10.7605/gdlxb.2012.03.011

Wang, Z. Q. (1991). Advances on the permo-triassic lycopods in North China. I. An Isoetes from the mid-Triassic in northern Shaanxi Province. *Palaeontogr. Abt. B* 222 (1–3), 1–30.

Warrington, G. (1979). A derived late permian palynomorph assemblage from the Keuper marl (late triassic), of west somerset. *Proc. Ussher Soc.* 4 (3), 299–302.

Warrington, G. (1970). "Palynology of the trias of the langford lodge borehole," in *Geology of belfast and the lagan valley*. Editors P. I. Manning, J. A. Robbie, H. E. Wilson, and E. Hull (Geological Survey of Northern Ireland), 44–51.

Wilson, K. M., Pollard, D., Hay, W. W., Thompson, S. L., and Wold, C. N. (1994). *General circulation model simulations of Triassic climates: Preliminary Results*, 288. Special Paper of the Geological Society of America, 91–116. doi:10.1130/SPE288-p91

Xie, X. Y., and Heller, P. L. (2013). U-Pb detrital zircon geochronology and its implications: The early late triassic Yanchang Formation, south Ordos Basin, China. *J. Asian Earth Sci.* 64, 86–98. doi:10.1016/j.jseaes.2012.11.045

Xu, Y. L., and Zhang, W. P. (1980). "Jurassic spores and pollen," in *Institute of Geology, Chinese academy of geological SciencesMesozoic stratigraphy and palaeontology of the shaanxi-gansu-ningxia basin* (Beijing: Geological Publishing House Press), 1, 144–186. (in Chinese).

Yang, R. C., Jin, Z. J., van Loon, A. J., Han, Z. Z., and Fan, A. P. (2017). Climatic and tectonic controls of lacustrine hyperpycnite origination in the Late Triassic Ordos Basin, central China: Implications for unconventional petroleum development. *AAPG Bull.* 101, 95–117. doi:10.1306/06101615095

Yang, S. R., Liu, J., and Zhang, M. F. (1995). Conodonts from the "Falang Formation" of southwestern Guizhou and their age. *J. Stratigr.* 19 (3), 161–198. (in Chinese with English abstract). doi:10.19839/j.nki.dcxzz.1995.03.001

Zhang, J. G., Lenz, O. K., Wang, P. J., and Hornung, J. (2021a). The eco-plant model and its implication on Mesozoic dispersed sporomorphs for bryophytes, pteridophytes, and gymnosperms. *Rev. Palaeobot. Palynology* 293, 104503. doi:10.1016/j.revpalbo.2021.104503

Zhang, K., Liu, R., Liu, Z. J., and Li, L. (2021b). Geochemical characteristics and geological significance of humid climate events in the Middle-Late Triassic (Ladinian-Carnian) of the Ordos Basin, central China. *Mar. Petroleum Geol.* 131 (5), 105179. doi:10.1016/j.marpetgeo.2021.105179

Zhang, L. J. (1984). "Late Triassic spores and pollen from central Sichuan," in *Palaeontologia sinica* (Beijing: Science Press). (in Chinese with English abstract).

Zhang, R., Jin, Z. J., Liu, Q. Y., Li, P., Huang, Z. K., Shi, J. Y., et al. (2019). Astronomical constraints on deposition of the Middle Triassic chang 7 lacustrine shales in the Ordos Basin, central China. *Palaeogeogr. Palaeoclimatol. Palaeoecol.* 528, 87–98. doi:10.1016/j.palaeo.2019.04.030

Zhao, X. D., Zheng, D. R., Xie, G. W., Jenkyns, H. C., Guan, C. G., Fang, Y. N., et al. (2020). Recovery of lacustrine ecosystems after the end-Permian mass extinction. *Geology* 48 (6), 609–613. doi:10.1130/G47502.1

Zhu, Z. C., Kuang, H. W., Liu, Y. Q., Benton, M. J., Newell, A. J., Xu, H., et al. (2020). Intensifying aeolian activity following the end-Permian mass extinction: Evidence from the Late Permian–Early Triassic terrestrial sedimentary record of the Ordos Basin, North China. *Sedimentology* 67, 2691–2720. doi:10.1111/sed.12716